New (η-C_5Me_5)M(PR_2)$_x$ Complexes (M = Ta, Mo, and W): Reversible P-H Bond Activation, sp^3 C-H Bond Activation, and P-C Bond Formation†

R. Thomas Baker,* Joseph C. Calabrese, Richard L. Harlow, and Ian D. Williams

Central Research and Development, Science and Engineering Laboratories, E. I. du Pont de Nemours and Co., Wilmington, Delaware 19880-0328

Received August 17, 1992

Reduction of Cp*$MCl_4(PMe_3)$ (Cp* = η-C_5Me_5, M = Mo, W) with 3 equiv of Na/Hg amalgam in the presence of 1 equiv of PMe_3 under nitrogen gives dinitrogen complex Cp*$MoCl(N_2)(PMe_3)_2$ (**1**) and metalated-phosphine complex Cp*$WHCl(PMe_3)(\eta^2$-$CH_2PMe_2)$ (**3**) in good yield. The molecular structure of **1**, determined by X-ray diffraction, consists of a square-pyramidal geometry about Mo with "trans" PMe_3 ligands. A similar structure is found for paramagnetic Cp*$MoCl_2(PMe_3)_2$, which is obtained using 2 equiv of Na/Hg. The molecular structure of **3** is also a "four-legged piano stool", with H trans to Cl and with the C atom of the $(CH_2PMe_2)^-$ ligand located between the two P atoms in the P-W-P plane. Complexes **1** and **3** are both good preparative sources of 16e⁻ "[Cp*$MCl(PMe_3)_2$]", as shown by their reaction with $P(OMe)_3$ to give Cp*$MCl[P(OMe)_3]_n(PMe_3)_{3-n}$ (n = 1, 2). While **1** reacts with $LiPR_2$ (R = Ph, cyclohexyl) to form Cp*$Mo(PR_2)(PMe_3)_2$ (**5a,b**) with a Mo-P double bond, **3** affords a novel divalent product, $(C_5Me_4CH_2PR_2)WH(PMe_3)_2$ (**6a,b**) resulting from sp^3 C-H bond activation and subsequent P-C bond formation. The molecular structure of **6b** consists of a distorted four-legged piano stool with H trans to the PCy_2 arm of the $(C_5Me_4CH_2PCy_2)^-$ ligand. Oxidative addition of PPh_2H to complexes **1** and **3** gives Cp*$MHCl(PPh_2)(PMe_3)$, which react in turn with $LiPPh_2$ to afford divalent Cp*$Mo(PPh_2)(PPh_2H)(PMe_3)$ (**5c**) and tetravalent Cp*$WH(PPh_2)_2(PMe_3)$ (**8a**). Substitution of PMe_3 in **8a** by PPh_2H gives divalent Cp*$W(PPh_2)(PPh_2H)_2$ (**5e**). In solution, tetravalent **8a,b** are in equilibrium with their divalent tautomers **5d,e** as a result of *reversible P-H bond activation*. The molecular structure of **8a** shows that the PC^{ipso}_2 planes of the terminal $(PPh_2)^-$ ligands are pseudoparallel to the C_5Me_5 ring plane and constitute a delocalized P-W-P unit with W-P bond orders of 1.5. Reaction of Cp*$TaMe_2(\eta$-$C_2H_4)$ with PPh_2H gives methane and Cp*$TaMe(PPh_2)(\eta$-$C_2H_4)$ (**9**); barriers to rotation about Ta-P and Ta-olefin bonds were estimated from ^{13}C DNMR spectra. Hydrogenation of **9** in the presence of PPh_2H affords methane, ethane, and fluxional complex Cp*$TaH(PPh_2)_3$, which contains two types of Ta-P multiple bonds.

In the course of preparing a wide variety of early-transition-metal complexes containing terminal diorganophosphide $(PR_2)^-$ ligands,[1-3] we found it useful to react low- or intermediate-oxidation-state metal halides with the $LiPR_2$ reagent, thus favoring halide/$(PR_2)^-$ metathesis over metal reduction and P_2R_4 formation. For the synthesis of (pentamethylcyclopentadienyl)molybdenum and -tungsten PR_2 complexes, we sought divalent precursors and chose to study the reduction of easily obtained tetrachlorides [Cp*MCl_4]$_n$ (Cp* = η-C_5Me_5) reported previously by Schrock et al.[4] This report describes results obtained with the PMe_3 ligand and includes two "stabilized" forms of 16e⁻ "[Cp*$MCl(PMe_3)_2$]" and their reactions with $P(OMe)_3$, PPh_2H, and $LiPR_2$ (R = Ph, cyclohexyl). Some related Cp*Ta chemistry is also presented. Several of the resulting products are useful metallo ligands for the construction of unsaturated, bis(PPh_2)-bridged, early-late heterobimetallics. A portion of this work has been reported previously.[5]

Experimental Section

All manipulations were performed in a nitrogen-filled Vacuum Atmospheres Dri-Lab glovebox or on a conventional high-vacuum line. Solvents were purified by standard techniques[6] and distilled under argon from sodium- or potassium-benzophenone ketyl. Literature procedures were used to prepare $LiPCy_2$,[7] $LiPPh_2$·dioxane,[7] Cp*$MCl_4(PMe_3)$ (M = Mo, W),[4] and Cp*$TaMe_2(\eta$-$C_2H_4)$.[8] As details of the latter are limited to a Ph.D. thesis, we have reproduced them below with the author's permission. All other chemicals were from commercial sources. NMR spectra were obtained on Nicolet NT-360 wide bore (360 MHz ^1H and 146 MHz ^{31}P), Nicolet NMC-300 wide-bore (300 MHz ^1H, 120.5 MHz ^{31}P and 75.5 MHz ^{13}C), and Nicolet QM-300 narrow-bore (300 MHz ^1H) spectrometers. ^{13}C and ^{31}P NMR chemical shifts are positive downfield from external $SiMe_4$ and 85% H_3PO_4, respectively. ESR spectra were recorded on a Bruker ER420 spectrometer equipped with a field-tracking gauss meter for accurate determination of g values. IR spectra were obtained as Nujol mulls on NaCl or CsI plates on a Perkin-Elmer 983 spectrometer. Elemental analysis was performed by Pascher

† Contribution No. 6125.

(1) $Cp_2M(PR_2)_x$: (a) (M = Ti, Zr, Hf) Baker, R. T.; Whitney, J. F.; Wreford, S. S. *Organometallics* **1983**, *2*, 1049; *Inorg. Chem.*, submitted for publication. (b) (M = Sc, Y, Lu) Baker, R. T.; Calabrese, J. C.; Glassman, T. E. *Organometallics*, manuscript in preparation.

(2) Cp*$M(PR_2)_x$ (M = Ti, Zr, Hf): Baker, R. T.; Krusic, P. J.; Calabrese, J. C.; Ortiz, J. V. *Organometallics*, manuscript in preparation.

(3) $M_x(PR_2)_y$: Baker, R. T.; Calabrese, J. C.; Krusic, P. J.; Tulip, T. H.; Wreford, S. S. *J. Am. Chem. Soc.* **1983**, *105*, 6763.

(4) Murray, R. C.; Blum, L.; Liu, A.; Schrock, R. R. *Organometallics* **1985**, *4*, 953.

(5) Baker, R. T.; Calabrese, J. C.; Harlow, R. L.; Williams, I. D. Third Chemical Congress of North America, Toronto, Canada, June 1988. Abstract INOR 80.

(6) Gordon, A. J.; Ford, R. A. *The Chemist's Companion*; Wiley Interscience: New York, 1972; Perrin, D. D.; Armarego, W. L. F.; Perrin, D. R. *Purification of Laboratory Chemicals*, 2nd ed.; Pergamon Press: Oxford, 1980.

(7) Issleib, K.; Tzschach, A. *Chem. Ber.* **1959**, *92*, 1118.

(8) McLain, S. J. Ph.D. Thesis, 1979, Massachusetts Institute of Technology, Cambridge, MA; Univ. Microfilms Intern., Ann Arbor, MI.

0276-7333/93/2312-0830$04.00/0

Table I. Elemental Analyses[a]

Complex	no.	% C	% H	% P	% M
$Cp^*MoCl(N_2)(PMe_3)_2$[b]	1	43.13, 43.08 (43.01)	7.47, 7.49 (7.44)	14.0, 14.0 (13.87)	21.7, 21.7 (21.47)
$Cp^*WHCl(PMe_3)(\eta$-$CH_2PMe_2)$[c]	3	37.77, 37.83 (37.93)	6.55, 6.56 (6.56)	11.2, 11.5 (12.23)	36.3, 36.9 (36.28)
$Cp^*Mo(PPh_2)(PMe_3)_2$[d]	5a	55.14, 52.08 (59.16)	7.57, 7.58 (7.62)	15.8, 15.0 (16.34)	18.3, 18.6 (16.88)
$(C_5Me_4CH_2PPh_2)WH(PMe_3)_2$	6a	51.16, 50.99 (50.48)	6.65, 6.56 (6.43)	13.1, 13.4 (14.46)	28.0, 28.6 (28.62)
$(C_5Me_4CH_2PCy_2)WH(PMe_3)_2$	6b	50.30, 50.16 (49.55)	8.45, 8.44 (8.16)	13.3, 13.2 (14.20)	27.6, 28.0 (28.09)
$Cp^*MoHCl(PPh_2)(PMe_3)$[e]	7a	56.69, 56.65 (56.77)	6.69, 6.73 (6.67)	11.7, 11.8 (11.71)	18.1, 18.1 (18.14)
$Cp^*WHCl(PPh_2)(PMe_3)$[f]	7b	48.86, 48.65 (48.68)	5.78, 5.72 (5.72)	10.1, 10.0 (10.04)	29.7, 30.0 (29.81)
$Cp^*Mo(PPh_2)(PPh_2H)(PMe_3)$	5c	65.96, 66.08 (65.49)	6.81, 6.80 (6.68)	13.5, 13.4 (13.69)	13.5, 13.6 (14.14)
$Cp^*W(PPh_2)(PPh_2H)_2$	5e	62.81, 62.24 (63.02)	5.39, 5.44 (5.40)	9.95, 9.94 (10.60)	20.7, 21.3 (20.97)
$Cp^*WH(PPh_2)_2(PMe_3)$	8a	58.47, 58.36 (57.98)	6.02, 5.99 (5.92)	11.8, 12.0 (12.12)	23.3, 23.9 (23.98)
$Cp^*TaMe(PPh_2)(\eta$-$C_2H_4)$	9	55.30, 55.13 (55.15)	5.87, 5.91 (5.92)	5.78, 5.78 (5.69)	33.2, 33.6 (33.23)
$Cp^*TaH(PPh_2)_3$	10	63.35, 62.86 (63.31)	5.38, 5.34 (5.31)	9.77, 9.92 (10.65)	20.7, 20.7 (20.73)

[a] Found; calculated values in parentheses. [b] % Cl: 9.38, 9.38 (7.93); % N: 4.98, 4.80 (6.27). These numbers reflect contamination due to $Cp^*MoCl_2(PMe_3)_2$ (ca. 20%). [c] % Cl: 6.86, 6.95 (7.00). [d] Low values of C, H, and P reflect some PMe_3 loss in vacuo. [e] % Cl: 6.87, 6.88 (6.70). [f] % Cl: 5.89, 5.90 (5.75).

Mikroanalytisches Labor, Remagen, Germany. Analytical and NMR spectroscopic data for all new compounds are listed in Tables I–IV, and complete IR spectroscopic data are included with the supplementary material.

Synthesis. $Cp^*TaMe_2(\eta$-$C_2H_4)$. Solid $LiCp^*$ (2.91 g, 20.5 mmol) was added to a solution of $TaCl_2Me_3$[42] (6.07 g. 20.4 mmol) in 80 mL of diethyl ether with vigorous stirring. The mixture was stirred for 2 h and filtered. The solvent was removed in vacuo and the residue dissolved in a minimal amount of toluene and filtered. Addition of pentane and cooling at −30 °C gave 6.38 g (79%) of $Cp^*TaClMe_3$. This solid (16.1 mmol) was dissolved in 150 mL of diethyl ether, and a benzene solution of EtLi (16.0 mL, 1.05 M) was added dropwise at −78 °C. After the addition was complete, the solution was warmed slowly to 25 °C and the color changed from orange to red with evolution of methane. The mixture was then filtered, the solvent was removed in vacuo, and the resulting red oil was extracted into pentane, filtered, and cooled at −30 °C to give red needles of $Cp^*TaMe_2(\eta$-$C_2H_4)$ (three crops totaled 3.26 g, 54%).

$Cp^*MoCl(N_2)(PMe_3)_2$, 1. To a solution of 9.0 g (20 mmol) $Cp^*MoCl_4(PMe_3)$ and 1.9 g (25 mmol) PMe_3 in 200 mL of THF was added 201.4 g of 0.7% Na/Hg amalgam (61 mmol). The solution turned red-brown and then blue-green. After stirring for 20 h the solution was filtered through Celite and evaporated in vacuo. The residue was extracted with 200 mL of hexane and concentrated to 50 mL in vacuo, and the resulting blue crystals were filtered off, washed with 2 × 10 mL of cold (−30 °C) pentane and dried in vacuo, yielding 4.13 g. Additional crops brought the total yield of 1 to 7.27 g (81%). The product was invariably contaminated with paramagnetic $Cp^*MoCl_2(PMe_3)_2$ (2), which cocrystallizes with 1. This impurity can be eliminated by using 3.5 equiv of Na/Hg, but the yield of 1 is reduced due to formation of an unidentified green product.

$Cp^*MoCl_2(PMe_3)_2$, 2. This complex was prepared as for 1 by using only 2 equiv of Na/Hg amalgam. Workup was identical, yielding red-brown crystals of 2 in 80% yield.

$Cp^*WHCl(PMe_3)(\eta$-$CH_2PMe_2)$, 3. To a solution of 5.52 g (10.3 mmol) $Cp^*WCl_4(PMe_3)$ and 1.17 g (15.4 mmol) PMe_3 in 150 mL of THF was added 93.3 g of 0.8% Na/Hg amalgam (30.9 mmol). The solution turned red-brown and then orange. After stirring for 20 h, the solution was filtered through Celite and evaporated in vacuo. The residue was extracted with 200 mL of hexane and cooled at −30 °C for 14 h. The resulting orange crystals were filtered off, washed with 10 mL of cold pentane, and vacuum-dried, yielding 3.36 g. Additional crops brought the total yield of 3 to 4.67 g (89%).

Generation of $Cp^*MCl[P(OMe)_3]_n(PMe_3)_{3-n}$ (M = Mo (W); n = 1, 4a (4c); n = 2, 4b (4d)). A solution of 62 mg (0.5 mmol) $P(OMe)_3$ in 10 mL of THF was added to a solution of 223 mg (0.5 mmol) $Cp^*MoCl(N_2)(PMe_3)_2$ in 20 mL of THF. The solution slowly turned red-purple, and the ^{31}P NMR spectra indicated a mixture of un-, mono-, and disubstituted complexes. An additional 62 mg $P(OMe)_3$ was then added and the tube gently heated to drive off PMe_3 and convert the mixture completely to $Cp^*MoCl[P(OMe)_3]_2(PMe_3)$, 4b, thus permitting ^1H and ^{31}P NMR spectroscopic characterization of 4a,b.

The W analogs 4c,d were generated similarly from 51 mg (0.1 mmol) $Cp^*WHCl(PMe_3)(\eta$-$CH_2PMe_2)$ and two successive aliquots of 12 mg (0.1 mmol) $P(OMe)_3$ in 1 mL of toluene-d_8. The products were characterized by ^1H and ^{31}P NMR spectroscopy.

$Cp^*Mo(PPh_2)(PMe_3)_2$, 5a. A solution of 850 mg (3.03 mmol) $LiPPh_2$·dioxane in 30 mL of THF was added dropwise to a solution of 1.34 g (3.0 mmol) $Cp^*MoCl(N_2)(PMe_3)_2$ in 30 mL of THF. After 20 h the resulting green solution was evaporated in vacuo and the residue was extracted with 200 mL of pentane and filtered. The filtrate was concentrated to 100 mL and cooled at −30 °C for 16 h. The resulting green crystals were filtered off, washed with cold pentane, and dried in vacuo to yield 669 mg. Additional crops brought the total yield of 5a to 1.084 g (64%).

The PCy_2 analog 5b was generated from 620 mg (3.04 mmol) $LiPCy_2$ and 1.34 g (3.0 mmol) $Cp^*MoCl(N_2)(PMe_3)_2$ as above, but contamination of the resulting green solids by P_2Cy_4 limited spectroscopic characterization of 5b to ^{31}P NMR spectroscopy.

$(C_5Me_4CH_2PPh_2)WH(PMe_3)_2$, 6a. A solution of 75 mg (0.27 mmol) $LiPPh_2$·dioxane in 10 mL of THF was added dropwise to a solution of 102 mg (0.2 mmol) $Cp^*WHCl(PMe_3)(\eta$-$CH_2PMe_2)$. After stirring for 2 days the solvent was removed in vacuo and the residue was extracted with 25 mL of hexane and filtered. The red-brown filtrate was concentrated to 10 mL and cooled at −30 °C for 14 h. The resulting brown crystals were filtered off and vacuum-dried to yield 75 mg 6a (58%).

The PCy_2 analog 6b was prepared similarly from 55 mg (0.27 mmol) $LiPCy_2$ and 102 mg (0.2 mmol) $Cp^*WHCl(PMe_3)(\eta$-$CH_2PMe_2)$ to give 9.0 mg brown orange crystals (69%).

$Cp^*MoHCl(PPh_2)(PMe_3)$, 7a. A solution of 1.45 g (7.8 mmol) PPh_2H in 10 mL of hexane was added to a solution of 1.74 g (3.9 mmol) $Cp^*MoCl(N_2)(PMe_3)_2$ in 100 mL of hexane and the mixture was heated at 60 °C for 20 hr. After the orange-brown solution

Table II. ^{1}H NMR Data[a]

complex	no.	chem shift (δ)[b] C_5Me_5	PMe_3	other
$Cp^*MoCl(N_2)(PMe_3)_2$[c]	**1**	1.54	1.18 (v tr, N = 16 Hz)	
$Cp^*MoCl_2(PMe_3)_2$	**2**	41.2 (br)	−2.0 (br)	
$Cp^*WHCl(PMe_3)(\eta\text{-}CH_2PMe_2)$[c]	**3**	2.01	1.32 (d, $^2J_{HP}$ = 12 Hz)	1.40, 1.36 (d, $^2J_{HP}$ = 12 Hz, 3H, PMe_2), 1.08 (app. q, J = 6.5 Hz, 1H, CH_2), 0.86 (d d d d, J = 2, 5, 5, 7 Hz, 1H, CH_2), −5.99 (d d d d, $^3J_{HH}$ = 4.5, 5.5 Hz, $^2J_{HP}$ = 13, 26 Hz, J_{HW} = 67 Hz, WH)
$Cp^*MoCl(PMe_3)_2[P(OMe)_3]$[c]	**4a**	1.70	1.43 (s, 18H)	3.19 (d, $^3J_{HP}$ = 10 Hz, 9H, $P(OMe)_3$)
$Cp^*MoCl(PMe_3)[P(OMe)_3]_2$[c]	**4b**	1.78	1.43 (s, 9H)	3.67, 3.28 (d, $^3J_{HP}$ = 10 Hz, 9H, $P(OMe)_3$)
$Cp^*WCl(PMe_3)_2[P(OMe)_3]$	**4c**	1.78	1.55 (m, 18H)	3.28 (d, $^3J_{HP}$ = 11 Hz, 9H, $P(OMe)_3$)
$Cp^*WCl(PMe_3)[P(OMe)_3]_2$	**4d**	1.85	1.55 (m, 9H)	3.68, 3.36 (d, $^3J_{HP}$ = 10.5 Hz, 9H, $P(OMe)_3$)
$Cp^*Mo(PPh_2)(PMe_3)_2$	**5a**	1.71	1.30 (v tr, N = 12 Hz)	7.38 (m, ortho), 7.12 (ov m, meta, para)
$Cp^*Mo(PCy_2)(PMe_3)_2$[c]	**5b**	1.92	1.34 (v tr, N = 12 Hz)	2.5–1.0 (ov m, PCy_2)
$(C_5Me_4CH_2PPh_2)WH(PMe_3)_2$	**6a**		1.39 (d, $^2J_{HP}$ = 5 Hz)	7.48 (m, ortho), 7.28 (ov m, meta, para), 3.58, 3.43 (d, 7, CH_2), 2.46, 2.09 (s, 6 H, C_5Me_4), −5.69 (tr d, $^2J_{HP}$ = 57 (cis), 13 Hz (trans), J_{HW} = 55 Hz, WH)
$(C_5Me_4CH_2PCy_2)WH(PMe_3)_2$[c]	**6b**		1.69 (d, $^2J_{HP}$ = 5 Hz)	2.46, 2.26 (s, 6H, C_5Me_4), 2.73 (d, 6, 2H, H_α of PCy_2), 2.0–1.0 (ov m, 22H, PCy_2 and obscured CH_2), −6.06 (tr d, $^2J_{HP}$ = 58 (cis), 12.5 Hz (trans), J_{HW} = 54 Hz, WH)
$Cp^*MoHCl(PPh_2)(PMe_3)$	**7a**	1.75	1.22 (d, $^2J_{HP}$ = 8 Hz)	7.71 (m, ortho), 7.30 (ov m, meta, para), −3.29 (d d, $^2J_{HP}$ = 95, 54.5 Hz, MoH)
$Cp^*WHCl(PPh_2)(PMe_3)$	**7b**	1.92	1.37 (d, $^2J_{HP}$ = 8.5 Hz)	7.62 (m, ortho), 7.28 (ov m, meta, para), −3.12 (d d, $^2J_{HP}$ = 83, 44 Hz, J_{HW} = 35 Hz, WH)
$Cp^*Mo(PPh_2)(PPh_2H)(PMe_3)$	**5c**	1.57	1.06 (d, $^2J_{HP}$ = 7 Hz)	8.31 (d d, J_{HP} = 306 Hz, $^3J_{HP}$ = 6 Hz, PH), 7.55, 7.49 (m, 2H, ortho), 7.27 (ov m, 6 H, ortho, meta), 7.19 (m, 4H, meta), 7.11 (ov m, 6H, meta, para)
$Cp^*W(PPh_2)(PPh_2H)(PMe_3)$[c]	**5d**	2.11	1.26 (d, $^2J_{HP}$ = 7.5 Hz)	10.34 (d d, J_{HP} = 316 Hz, $^3J_{HP}$ = 6 Hz, PH), 7.58, 7.47 (m, 2H, ortho), 7.29 (ov m, 6H, ortho, meta), 7.15 (m, 4H, meta), 7.09 (ov m, 6H, meta, para)
$Cp^*W(PPh_2)(PPh_2H)_2$[c]	**5e**	1.77		10.09 (d d, J_{HP} = 328 Hz, $^3J_{HP}$ = 14.5 Hz, PH), 7.62, 7.48, 7.38 (m, 4H, ortho, meta of PPh_2 and PPh_2H), 7.1–6.9 (ov m, meta, para of PPh_2 and PPh_2H)
$Cp^*WH(PPh_2)_2(PMe_3)$[c]	**8a**	1.83	1.16 (d, $^2J_{HP}$ = 8 Hz)	7.54 (m, ortho), 7.19 (m, meta), 7.07 (m, para), 0.98 (tr d, $^2J_{HP}$ = 61, 14 Hz, WH)
$Cp^*TaMe(PPh_2)(\eta\text{-}C_2H_4)$	**9**	1.66		7.51 (tr, 7, ortho), 7.17 (tr, 7, meta), 7.06 (tr, 7, para), 2.36, 1.92, 0.70, 0.40 (br, 1H, C_2H_4), −0.95 (d, $^3J_{HP}$ = 9 Hz, TaMe)
at −80 °C in toluene-d_8		1.57		7.62 (tr, 7, ortho), 7.43 (tr, 7, ortho), 7.3–6.9 (ov m, meta and para), 2.25, 1.75, 1.25, 0.50 (m, 1H, C_2H_4), −0.93 (d, $^3J_{HP}$ = 8 Hz, TaMe)
$Cp^*TaH(PPh_2)_3$	**10**	1.91		9.90 (q, $^2J_{HP}$ = 65 Hz, TaH), 7.43 (m, 12H, ortho), 7.18 (m, 12H, meta), 7.08 (m, 6H, para)
at −90 °C		1.81		9.47 (tr d, $^2J_{HP}$ = 84, 25 Hz, TaH), 7.71 (m, 4H, ortho), 7.64 (m, 8H, ortho), 7.4–7.0 (ov m, 18H, meta, para)

[a] Recorded at 25 °C in THF-d_8. [b] Multiplicity: s = singlet, d = doublet, tr = triplet, q = quartet, ov = overlapping, m = multiplet, br = broad, app = apparent, v = virtual. N = $^2J_{PH}$ + $^4J_{PH}$ = separation of outer lines of virtual triplet. [c] Recorded in C_6D_6.

Table III. ^{31}P NMR Data[a]

complex	no.	chem shift[b] (ppm)
$Cp^*MoCl(N_2)(PMe_3)_2$[c]	**1**	14.7
$Cp^*WHCl(PMe_3)(\eta\text{-}CH_2PMe_2)$[c]	**3**	−29.7 (d, 13.5, J_{PW} = 257 Hz), −56.6 (d, J_{PW} = 214 Hz)
$Cp^*MoCl(PMe_3)_2[P(OMe)_3]$	**4a**	210.5 (tr, 98), 15.8 (d)
$Cp^*MoCl(PMe_3)[P(OMe)_3]_2$	**4b**	208.9 (d d, 125, 103), 195.7 (d d, 125, 27), 9.3 (d d, 103, 27)
$Cp^*WCl(PMe_3)_2[P(OMe)_3]$[d]	**4c**	165.2 (tr, 64, J_{PW} = 572 Hz), 25.0 (d, J_{PW} = 317 Hz)
$Cp^*WCl(PMe_3)[P(OMe)_3]_2$[d]	**4d**	166.1 (d d, 87, 72, J_{PW} = 580 Hz), 154.8 (d d, 87, 42, J_{PW} = 527 Hz), −28.6 (d d, 72, 42, J_{PW} = 282 Hz)
$Cp^*Mo(PPh_2)(PMe_3)_2$	**5a**	161.3 (tr, 38.5), 20.7 (d)
$Cp^*Mo(PCy_2)(PMe_3)_2$[c]	**5b**	238.7 (tr, 40), 25.8 (d)
$(C_5Me_4CH_2PPh_2)WH(PMe_3)_2$	**6a**	−34.4 (d, 37, J_{PW} = 333 Hz), −84.3 (tr, J_{PW} = 229 Hz)
$(C_5Me_4CH_2PCy_2)WH(PMe_3)_2$[c]	**6b**	−34.9 (d, 34.5, J_{PW} = 347 Hz), −89.8 (tr, J_{PW} = 174 Hz)
$Cp^*MoHCl(PPh_2)(PMe_3)$	**7a**	220.2 (d, 21, PPh_2), 3.07 (d, PMe_3)
$Cp^*WHCl(PPh_2)(PMe_3)$	**7b**	145.1 (s, J_{PW} = 558 Hz, PPh_2), −13.7 (s, J_{PW} = 239 Hz, PMe_3)
$Cp^*Mo(PPh_2)(PPh_2H)(PMe_3)$	**5c**	177.1 (d d, 48, 38, PPh_2), 67.1 (tr, 37, PPh_2H), 18.2 (d d, 48, 36, PMe_3)
$Cp^*W(PPh_2)(PPh_2H)(PMe_3)$	**5d**	137.4 (d d, 22, 14, J_{PW} = 643 Hz, PPh_2), 15.0 (tr, 12, J_{PW} = 454 Hz, PPh_2H), −36.3 (d d, 22, 12, J_{PW} = 383 Hz, PMe_3)
$Cp^*W(PPh_2)(PPh_2H)_2$	**5e**	155.2 (tr, 20, J_{PW} = 640 Hz, PPh_2), 35.3 (d, J_{PW} = 396 Hz, PPh_2H)
$Cp^*WH(PPh_2)_2(PMe_3)$	**8a**	98.8 (d, 29, J_{PW} = 369 Hz, PPh_2), −28.2 (tr, J_{PW} = 282 Hz, PMe_3)
$Cp^*WH(PPh_2)_2(PPh_2H)$	**8b**	105.8 (d, 37, J_{PW} = 350 Hz, PPh_2), 27.5 (tr, J_{PW} = 284 Hz, PPh_2H)
$Cp^*TaMe(PPh_2)(\eta\text{-}C_2H_4)$	**9**	170.3
$Cp^*TaH(PPh_2)_3$[d,e]	**10**	169.0 (br, $\Delta\nu_{1/2}$ = 850 Hz)
at −80 °C		253.2 (tr, 59, 1P), 119.6 (d, 2P)

[a] Recorded at 25 °C in THF-d_8. [b] Multiplicity, $^2J_{PP}$ in Hz in parentheses. [c] Recorded in C_6D_6. [d] In toluene-d_8. [e] At 110 °C.

was cooled to ambient temperature, the resulting solid was filtered off, washed with 2 × 5 mL of hexane, and dried in vacuo to give 707 mg orange-brown, microcrystalline solid. Concentration of the filtrate to 10 mL gave a second crop of 520 mg, bringing the total yield of **7a** to 1.227 g (59%).

The W analog **7b** was prepared similarly from 600 mg (3.2 mmol) PPh_2H and 1.22 g (2.4 mmol) $(C_5Me_5)WHCl(PMe_3)(\eta\text{-}CH_2PMe_2)$ to give 1.097 g green microcrystalline solid (74%).

$Cp^*Mo(PPh_2)(PPh_2H)(PMe_3)$, 5c. A solution of 160 mg (0.57 mmol) $LiPPh_2$·dioxane in 20 mL of THF was added dropwise to

Table IV. ^{13}C NMR Data[a]

complex	no.	chem shift (ppm) C_5Me_5	PR_2	other
$Cp^*MoCl(N_2)(PMe_3)_2$	**1**	101.6 (s), 10.8 (q, 126)		15.0 (q v tr, 126, $J_{CP} = {}^3J_{CP} =$ 11 Hz)
$Cp^*WHCl(PMe_3)(\eta$-$CH_2PMe_2)$[b]	**3**	93.3 (s), 13.1 (d, $^3J_{CP} =$ 2 Hz)		18.6 (d d, $J_{CP} = 27$ Hz, $^3J_{CP} =$ 1 Hz, 3C, CH_3), 17.9 (d d, $J_{CP} = 37$ Hz, $^3J_{CP} = 3$ Hz, 1C, CH_3), 13.7 (d d, $J_{CP} = 14$ Hz, $^2J_{CP} = 7$ Hz, 1C, CH_2), 3.2 (d, $J_{CP} = 24$ Hz, 1C, CH_3)
$Cp^*Mo(PPh_2)(PMe_3)_2$[b,c]	**5a**	101.6, 13.8 (s)	134 (s, 2C, ipso), 131.6 (s, 4C, ortho), 127.8 (s, 4C, meta), 126.9 (s, 2C, para)	30.0 (v tr d, $J_{CP} = {}^3J_{CP} = 11$ Hz, $^3J_{CP'} = 3$ Hz)
$(C_5Me_4CH_2PCy_2)WH(PMe_3)_2$[b]	**6b**	88.7, 83.1 (s, 2C), 74.4 (s, 1C), 16.2, 15.5 (s, 2C, CH_3)	44.8 (d, $J_{CP} = 4$ Hz, 2C, Cα), 30.9, 30.0, 27.0 (s, 2C, CH_2 of Cy), 28.3 (ov m, 5C, CH_2 of Cy and $C_5Me_4CH_2PCy_2$)	33.2 (m, 6C, CH_3)
$Cp^*MoHCl(PPh_2)(PMe_3)$[c]	**7a**	103.8 (s), 12.7 (q, 127)	151.0 (d, $J_{CP} = 8.5$ Hz, 2C, ipso), 133.1 (d d, 160, $^2J_{CP} = 7.5$ Hz, 4C, ortho), 128.6 (d d, 163, $^4J_{CP} = 4$ Hz, 2C, para), 128.2 (d d, 160, $^3J_{CP} = 10$ Hz, 4C, meta)	20.9 (q d, 129, $J_{CP} = 27$ Hz, 3C, CH_3)
$Cp^*WHCl(PPh_2)(PMe_3)$[b,c]	**7b**	102.2, 13.0 (s)	156.2 (d, $J_{CP} = 19$ Hz, 2C, ipso), 133.1 (m, 4C, ortho), 128.3 (s, 2C, para), 128.2 (m, 4C, meta)	22.4 (d d, $J_{CP} = 31$ Hz, $^3J_{CP} =$ 1 Hz, 3C, CH_3)
$Cp^*TaMe(PPh_2)(\eta$-$C_2H_4)$[d]	**10**	114.5 (s), 11.7 (q, 127)	152.1 (s, 1C, ipso), 145.9 (d, $J_{CP} = 41$ Hz, 1C, ipso), 136.9 (d, 162, 2C, ortho), 132.5 (d, 161, 2C, ortho), 128.8 (d, 159, 2C, meta), 128.1 (ov d, 161, 3C, meta and para), 127.3 (d, 159, 1C, para)	58.5 (tr, 147, 1C, CH_2), 51.3 (q, 119, 1C, CH_3), 46.6 (tr d, 157, $^2J_{CP} = 11$ Hz, 1C, CH_2)

[a] Recorded at 25 °C in C_6D_6 with gated decoupling; multiplicity and J_{CH} in Hz in parentheses; see Table II for abbreviations. [b] Proton-decoupled. [c] Recorded in THF-d_8. [d] Recorded at −95 °C in THF-d_8.

a solution of 251 mg (0.47 mmol) $Cp^*MoHCl(PPh_2)(PMe_3)$ in 25 mL of THF. The resulting green solution was evaporated in vacuo, extracted with 25 mL of hexane, and filtered. The filtrate was evaporated in vacuo to yield 243 mg **5c** (76%).

$Cp^*WH(PPh_2)_2(PMe_3)$, 8a. A solution of 273 mg (0.97 mmol) $LiPPh_2$·dioxane in 20 mL of THF was added dropwise to a cold (−80 °C) solution of 500 mg (0.8 mmol) $Cp^*WHCl(PPh_2)(PMe_3)$ in 30 mL of THF. After warming slowly (2 h) to ambient temperature, the resulting blue solution was evaporated in vacuo and the residue was extracted with 50 mL of hexane and filtered. After concentration of the filtrate with 5 mL and cooling at −30 °C for 16 h, the resulting blue crystals were filtered off, washed with 5 mL of cold pentane, and dried in vacuo to yield 288 mg. A second crop brought the total yield of **8a** to 499 mg (80%). The complex was recrystallized by slow evaporation of a concentrated Et_2O solution.

$Cp^*W(PPh_2)(PPh_2H)_2$, 5e. A solution of 135 mg (0.2 mmol) $Cp^*WH(PPh_2)_2(PMe_3)$, **8a**, and 33 mg (0.2 mmol) PPh_2H in 20 mL of THF was stirred in an open vessel for 3 days. After removal of the solvent in vacuo, the dark green residue was washed with cold pentane to yield 70 mg green solid **5e**. Additional crops brought the total yield to 105 mg (68%).

$Cp^*TaMe(PPh_2)(\mu$-$C_2H_4)$, 9. A solution of 709 mg (3.8 mmol) PPh_2H in 20 mL of hexane was added dropwise to a solution of 1.32 g (3.5 mmol) $Cp^*TaMe_2(\eta$-$C_2H_4)$ in 50 mL of hexane. After stirring for 14 h, the solution was concentrated to 15 mL and the resulting orange-brown microcrystalline solid was filtered off, washed with 2 × 5 mL of cold pentane, and dried in vacuo to yield 601 mg. After cooling the filtrate at −30 °C for 18 h, a second crop of 507 mg was isolated, bringing the total yield of **9** to 1.10 g (58%).

$Cp^*TaH(PPh_2)_3$, 10. A solution of 6.2 mmol $Cp^*TaMe(PPh_2)$-(η-C_2H_4), **9** (generated from 2.31 g (6.2 mmol) $Cp^*TaMe_2(\eta$-$C_2H_4)$ and 4.02 g (21.6 mmol) PPh_2H in 125 mL of THF), was treated with H_2 using a Schlenk tube and a balloon inflated to 6-in. diameter. The red solution turned purple. After 20 h the solvent was removed in vacuo and 25 mL of hexane was added to the residue. The resulting purple solid was filtered off, washed with 4 × 10 mL of hexane, and vacuum-dried to yield 4.34 g (81%). Purple plates of **10** were obtained by benzene–heptane recrystallization.

Molecular Structure Determination. Crystals suitable for X-ray diffraction were obtained as described above. A summary of the crystallographic results is presented in Table V. All data sets were collected at low temperatures on Enraf-Nonius CAD4 or Syntex R3 diffractometers using graphite-filtered Mo radiation. Data were reduced in the usual fashion for Lorentz–polarization, and absorption corrections were applied for **3** (empirical, range of transmission factors 0.812–1.00), **6b** (DIFABS,[9] 0.22–0.27), and **8a** (DIFABS, 0.40–0.81). Structure solution and refinement were performed on a VAX/IBM cluster system using a local program set. Heavy-atom positions were obtained via automated Patterson analysis and used to phase reflections for the remaining light atoms via the usual combination of structure factor, Fourier synthesis, and full-matrix least-squares refinement. All refinements were performed using full-matrix least squares on F, with anisotropic thermal parameters for all non-hydrogen atoms, and included anomalous dispersion terms[10] for Mo, W, Cl, and P, as well as idealized hydrogen coordinates as fixed atom contributors. For **3** and **6b** the W–H was directly located and successfully refined. For **8a** the W–H was not located from a low-angle (0–35°) Fourier difference map. A calculated position, suggested by the geometry about W, was adjusted with low-angle data and later refined normally with the complete data set. For **1**, the molecule is in a general position with a 2-fold disorder about the Mo–ring centroid axis. As a result of the superposition of N_2 and Cl^- ligands, the Mo–N, Mo–Cl, and N–N bond distances were not accurately determined. For acentric structures the enantiomorph was chosen on the basis of an R-value test. Selected bond distances and angles for **2**, **3**, **6b**, and **8a** are given in Tables VI–IX. Details of metal coordination geometries are presented in Table X. Tables of final positional and thermal parameters for non-hydrogen atoms, general temperature factors, and calculated hydrogen atom positions are available as supplementary material.

Results

Synthesis. Reduction of $Cp^*MCl_4(PMe_3)$ with 3 equiv of Na/Hg amalgam in THF in the presence of 1 equiv of PMe_3 under N_2 proceeds readily for M = Mo and W. For

(9) Walker, N.; Stuart, D. *Acta Cryst.* **1983**, *A39*, 158.
(10) Cromer, D. T.; Waber, J. T. *International Tables for X-ray Crystallography*; Kynoch Press: Birmingham, England, 1974; Vol. IV, Tables 2.2A, 2.31.

Table V. Summary of X-ray Diffraction Data

complex	Cp*MoCl(N$_2$)(PMe$_3$)$_2$ (1)	Cp*MoCl$_2$(PMe$_3$)$_2$ (2)	Cp*WHCl(PMe$_3$)-(η-CH$_2$PMe$_2$) (3)	(C$_5$Me$_4$CH$_2$PCy$_2$)-WH(PMe$_3$)$_2$ (6b)	Cp*WH(PPh$_2$)$_2$-(PMe$_3$) (8a)
formula	$C_{16}H_{33}ClMoN_2P_2$	$C_{16}H_{33}Cl_2MoP_2$	$C_{16}H_{33}ClP_2W$	$C_{28}H_{55}P_3W$	$C_{37}H_{45}P_3W$
fw	446.80	454.23	506.69	668.52	766.54
a, Å	8.700 (7)	14.446 (2)	14.628 (1)	19.028 (3)	11.410 (3)
b, Å	16.153 (20)	15.925 (2)	13.280 (1)	9.055 (2)	11.680 (3)
c, Å	15.428 (6)	9.072 (1)	10.178 (1)	35.046 (7)	15.794 (5)
α, deg					105.67 (3)
β, deg	101.25 (4)		92.33 (1)	93.82 (3)	96.94 (2)
γ, deg					117.39 (2)
V, Å^3	2126.4	2087.0	1975.7 (5)	6025.0	1723.9
Z	4	4	4	8	2
ρ_{calcd}, g cm^{-3}	1.395	1.445	1.703	1.474	1.477
space group	$P2_1/n$ (No. 14)	$P2_12_12_1$ (No. 19)	$P2_1/n$ (No. 14)	$I2/a$ (No. 15)	$P\bar{1}$ (No. 2)
cryst dimens, mm	0.45 × 0.35 × 0.30	0.39 × 0.31 × 0.40	0.34–0.35 (irreg sphere)	0.32 × 0.34 × 0.36	0.48 × 0.30 × 0.53
temp, °C	−70	−100	−100	−100	−70
radiation	Mo Kα	Mo Kα	Mo Kα	Mo Kα	Mo Kα
μ, cm^{-1}	8.77	10.17	62.6	40.88	35.82
data collection method	ω	ω	ω	ω	ω
max 2θ, deg	48.0	55.0	55.0	55.0	55.0
scan speed, deg/min	2.00–4.00	2.00–9.80	4–10	2.00–11.70	1.70–5.00
scan width, deg	1.5–1.7 ω	1.30 ω	1.00 ω	1.10 ω	1.20–2.00 ω
total no. of observns	5117	2765	5007	7503	8261
no. of unique data, $I > 3\sigma(I)$	2257	2521	3885	5440	6851
final no. of variables	256	190	280	293	374
final max shift/error	0.38	0.06	0.05	0.00	0.03
max residual density, e/Å^3	0.49	0.32	0.73	0.99	0.89
R^a	0.034	0.019	0.021	0.025	0.020
$R_w{}^b$	0.034	0.024	0.022	0.029	0.025

[a] $\sum||F_o| - |F_c||/\sum|F_o|$. [b] $[\sum w(|F_o| - |F_c|)^2/\sum wF_o^2]^{1/2}$.

Table VI. Selected Bond Distances (Å) and Angles (deg) for Cp*MoCl$_2$(PMe$_3$)$_2$ (2)

Mo(1)–Cl(1)	2.4841 (8)	P(2)–C(22)	1.820 (3)
Mo(1)–Cl(2)	2.4932 (7)	P(2)–C(23)	1.827 (3)
Mo(1)–P(1)	2.5104 (8)	C(1)–C(2)	1.413 (5)
Mo(1)–P(2)	2.5080 (8)	C(1)–C(5)	1.412 (4)
Mo(1)–C(1)	2.407 (3)	C(1)–C(6)	1.504 (5)
Mo(1)–C(2)	2.296 (3)	C(2)–C(3)	1.439 (4)
Mo(1)–C(3)	2.227 (3)	C(2)–C(7)	1.511 (4)
Mo(1)–C(4)	2.267 (3)	C(3)–C(4)	1.454 (4)
Mo(1)–C(5)	2.381 (3)	C(3)–C(8)	1.495 (4)
P(1)–C(11)	1.816 (4)	C(4)–C(5)	1.419 (4)
P(1)–C(12)	1.824 (4)	C(4)–C(9)	1.499 (4)
P(1)–C(13)	1.831 (3)	C(5)–C(10)	1.505 (4)
P(2)–C(21)	1.817 (4)		
Cl(1)–Mo(1)–Cl(2)	130.71 (3)	Mo(1)–P(2)–C(21)	119.2 (1)
Cl(1)–Mo(1)–P(1)	76.93 (3)	Mo(1)–P(2)–C(22)	110.3 (1)
Cl(1)–Mo(1)–P(2)	78.33 (3)	Mo(1)–P(2)–C(23)	119.2 (1)
Cl(2)–Mo(1)–P(1)	78.44 (3)	C(11)–P(1)–C(12)	101.0 (2)
Cl(2)–Mo(1)–P(2)	79.38 (3)	C(11)–P(1)–C(13)	101.7 (2)
P(1)–Mo(1)–P(2)	121.61 (3)	C(12)–P(1)–C(13)	100.1 (2)
P(1)–Mo(1)–C(1)	151.49 (8)	C(21)–P(2)–C(22)	100.8 (2)
Mo(1)–P(1)–C(11)	108.7 (1)	C(21)–P(2)–C(23)	102.7 (2)
Mo(1)–P(1)–C(12)	121.0 (1)	C(22)–P(2)–C(23)	101.9 (2)
Mo(1)–P(1)–C(13)	121.1 (1)		

Table VII. Selected Bond Distances (Å) and Angles (deg) for Cp*WHCl(PMe$_3$)(η-CH$_2$PMe$_2$) (3)

W–Cl	2.5508 (8)	P(2)–C(4)	1.821 (4)
W–P(1)	2.3464 (8)	P(2)–C(5)	1.828 (4)
W–P(2)	2.4805 (8)	P(2)–C(6)	1.829 (5)
W–C(1)	2.277 (3)	C(11)–C(12)	1.406 (4)
W–C(11)	2.394 (4)	C(11)–C(15)	1.419 (4)
W–C(12)	2.379 (3)	C(11)–C(16)	1.502 (5)
W–C(13)	2.263 (3)	C(12)–C(13)	1.427 (4)
W–C(14)	2.235 (3)	C(12)–C(17)	1.506 (4)
W–C(15)	2.300 (3)	C(13)–C(14)	1.443 (4)
W–HW	1.61 (4)	C(13)–C(18)	1.495 (4)
P(1)–C(1)	1.750 (3)	C(14)–C(15)	1.442 (4)
P(1)–C(2)	1.822 (4)	C(14)–C(19)	1.508 (4)
P(1)–C(3)	1.813 (4)	C(15)–C(20)	1.503 (4)
Cl–W–P(1)	89.07 (3)	C(1)–P(1)–C(2)	113.2 (2)
Cl–W–P(2)	84.03 (4)	C(1)–P(1)–C(3)	112.9 (2)
Cl–W–C(1)	79.63 (9)	C(2)–P(1)–C(3)	104.5 (3)
Cl–W–HW	149 (2)	W–P(2)–C(4)	114.1 (1)
P(1)–W–P(2)	121.05 (3)	W–P(2)–C(5)	116.9 (2)
P(1)–W–C(1)	44.45 (9)	W–P(2)–C(6)	122.5 (1)
P(1)–W–HW	82 (1)	C(4)–P(2)–C(5)	101.7 (2)
P(2)–W–C(1)	76.81 (9)	C(4)–P(2)–C(6)	100.1 (3)
P(2)–W–HW	76 (2)	C(5)–P(2)–C(6)	98.2 (2)
C(1)–W–HW	73 (2)	W–C(1)–P(1)	69.9 (1)
W–P(1)–C(1)	65.7 (2)	W–C(1)–H(1)A	114 (3)
W–P(1)–C(2)	125.5 (1)	W–C(1)–H(1)B	114 (4)
W–P(1)–C(3)	126.8 (1)		

M = Mo, dark blue crystals of dinitrogen complex Cp*MoCl(N$_2$)(PMe$_3$)$_2$ (1) are isolated, while for M = W, orange crystals of metalated-phosphine complex Cp*-WHCl(PMe$_3$)(η^2-CH$_2$PMe$_2$) (3) are obtained (Scheme I). While the W reaction is quantitative when monitored by ^{1}H and ^{31}P NMR spectroscopy, the Mo reaction is very sensitive to the amount of reducing agent employed; using 3 equiv Na/Hg gives product 1 which is invariably contaminated with the trivalent species[11] Cp*MoCl$_2$-(PMe$_3$)$_2$ (2). Pure samples of 1 and 2 (by ^{1}H NMR spectroscopy) were obtained using 3.5 and 2.0 equiv of Na/Hg, respectively. Complexes 1–3 were characterized by elemental analysis, IR and NMR spectroscopy (Tables I–IV and supplementary material), and single-crystal X-ray diffraction.

Molecular Structures of 1–3. The molecular structures of complexes 1 and 2 (Figure 1) both consist of a square-pyramidal Mo center with "trans" PMe$_3$ ligands and an apical (η-C$_5$Me$_5$) ring. The monoclinic form of 1 suffers from a 2-fold disorder which superposes the N$_2$ and Cl$^-$ ligands. This disorder, and probable cocrystallization of some 2 in the diffraction sample, prevented accurate determination of the Mo–N, Mo–Cl, and N–N bond distances. While the previously reported ordered structure[11] of the orthorhombic form of 1 suffered from

(11) A single crystal ESR study of complex 2 doped in crystals of 1 appeared recently: Baker, R. T.; Morton, J. R.; Preston, K. F.; Williams, A. J.; Le Page, Y. *Inorg. Chem.* **1991**, *30*, 113.

Table VIII. Selected Bond Distances (Å) and Angles (deg) for $(C_5Me_4CH_2PCy_2)WH(PMe_3)_2$ (6b)

W(1)–P(1)	2.387 (1)	P(2)–C(23)	1.849 (4)
W(1)–P(2)	2.400 (1)	P(3)–C(31)	1.890 (4)
W(1)–P(3)	2.515 (1)	P(3)–C(41)	1.878 (4)
W(1)–C(50)	2.293 (4)	P(3)–C(51)	1.854 (4)
W(1)–C(52)	2.317 (4)	C(50)–C(51)	1.512 (5)
W(1)–C(54)	2.271 (4)	C(50)–C(52)	1.424 (5)
W(1)–C(56)	2.274 (4)	C(50)–C(58)	1.442 (5)
W(1)–C(58)	2.339 (4)	C(52)–C(53)	1.492 (6)
W(1)–H(1)	1.72 (5)	C(52)–C(54)	1.428 (6)
P(1)–C(11)	1.842 (5)	C(54)–C(55)	1.501 (5)
P(1)–C(12)	1.848 (4)	C(54)–C(56)	1.445 (6)
P(1)–C(13)	1.837 (5)	C(56)–C(57)	1.501 (6)
P(2)–C(21)	1.844 (4)	C(56)–C(58)	1.434 (5)
P(2)–C(22)	1.850 (5)	C(58)–C(59)	1.493 (5)
P(1)–W(1)–P(2)	97.42 (4)	P(3)–W(1)–C(54)	120.7 (1)
P(1)–W(1)–P(3)	95.59 (3)	P(3)–W(1)–C(56)	122.9 (1)
P(2)–W(1)–P(3)	94.83 (3)	P(3)–W(1)–C(58)	88.0 (1)
P(1)–W(1)–C(50)	129.9 (1)	P(1)–W(1)–H(1)	67 (2)
P(1)–W(1)–C(52)	163.0 (1)	P(2)–W(1)–H(1)	77 (2)
P(1)–W(1)–C(54)	137.1 (1)	P(3)–W(1)–H(1)	160 (2)
P(1)–W(1)–C(56)	105.4 (1)	W(1)–P(1)–C(11)	116.9 (1)
P(1)–W(1)–C(58)	102.5 (1)	W(1)–P(1)–C(12)	119.3 (2)
P(2)–W(1)–C(50)	123.4 (1)	W(1)–P(1)–C(13)	122.4 (2)
P(2)–W(1)–C(52)	99.4 (1)	W(1)–P(2)–C(21)	115.5 (1)
P(2)–W(1)–C(54)	101.0 (1)	W(1)–P(2)–C(22)	123.4 (2)
P(2)–W(1)–C(56)	132.6 (1)	W(1)–P(2)–C(23)	120.3 (2)
P(2)–W(1)–C(58)	159.6 (1)	W(1)–P(3)–C(31)	120.6 (1)
P(3)–W(1)–C(50)	65.3 (1)	W(1)–P(3)–C(41)	130.6 (1)
P(3)–W(1)–C(52)	85.1 (1)	W(1)–P(3)–C(51)	88.0 (1)

Table IX. Selected Bond Distances (Å) and Angles (deg) for $Cp^*WH(PPh_2)_2(PMe_3)$ (8a)

W(1)–P(1)	2.476 (1)	P(1)–C(13)	1.827 (5)
W(1)–P(2)	2.325 (2)	P(2)–C(21)	1.822 (5)
W(1)–P(3)	2.322 (2)	P(2)–C(31)	1.840 (5)
W(1)–C(1)	2.418 (5)	P(3)–C(41)	1.828 (5)
W(1)–C(2)	2.382 (5)	P(3)–C(51)	1.836 (5)
W(1)–C(3)	2.305 (5)	C(1)–C(2)	1.423 (7)
W(1)–C(4)	2.298 (5)	C(1)–C(5)	1.404 (7)
W(1)–C(5)	2.378 (5)	C(2)–C(3)	1.424 (7)
W(1)–H(1)	1.55 (4)	C(3)–C(4)	1.428 (7)
P(1)–C(11)	1.820 (6)	C(4)–C(5)	1.406 (7)
P(1)–C(12)	1.820 (6)		
P(1)–W(1)–P(2)	87.91 (5)	C(11)–P(1)–C(12)	100.8 (3)
P(1)–W(1)–P(3)	86.41 (6)	C(11)–P(1)–C(13)	99.7 (3)
P(2)–W(1)–P(3)	113.76 (6)	C(12)–P(1)–C(13)	99.7 (3)
P(1)–W(1)–H(1)	151 (2)	C(21)–P(2)–C(31)	101.5 (2)
P(2)–W(1)–H(1)	78 (2)	C(41)–P(3)–C(51)	98.9 (2)
P(3)–W(1)–H(1)	76 (2)	P(2)–C(21)–C(22)	121.0 (4)
W(1)–P(1)–C(11)	119.6 (2)	P(2)–C(21)–C(26)	121.8 (4)
W(1)–P(1)–C(12)	115.8 (2)	P(2)–C(31)–C(32)	121.2 (4)
W(1)–P(1)–C(13)	117.8 (2)	P(2)–C(31)–C(36)	120.4 (4)
W(1)–P(2)–C(21)	127.3 (2)	P(3)–C(41)–C(42)	122.3 (4)
W(1)–P(2)–C(31)	131.1 (2)	P(3)–C(41)–C(46)	120.4 (4)
W(1)–P(3)–C(41)	124.3 (2)	P(3)–C(51)–C(52)	121.6 (4)
W(1)–P(3)–C(51)	136.0 (2)	P(3)–C(51)–C(56)	120.9 (4)

Scheme I

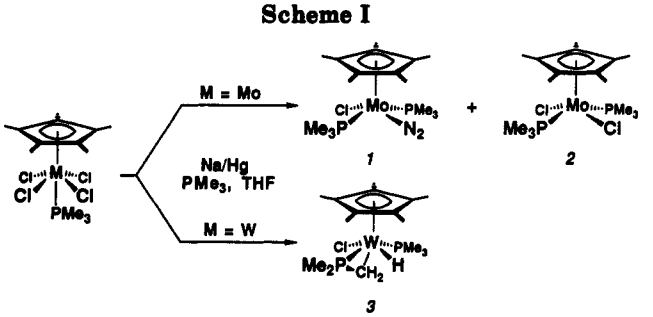

about 2% admixture of **2**, accurate details of Mo–P and Mo–Cp* ring bonding were obtained. The Mo–P bonds are ca. 0.04 Å longer in **2** (higher oxidation state) than in **1**, as also seen for the Mo(III/IV) pair $[CpMoCl_2(PMe_3)_2]^{0,+}$ by Poli et al.[12] Although the C–C bond distances of the $(C_5Me_5)^-$ ligand only vary from 1.41 to 1.45 Å, the Mo atom exhibits a pronounced "slip" distortion[13] with three Mo–C bond distances ca. 0.1 Å shorter than the other two in both **1** and **2**. The P1–W–P2 angle increases from 114.4° in **1** to 121.6° in **2**, presumably to accommodate the bulkier Cl^- ligand.

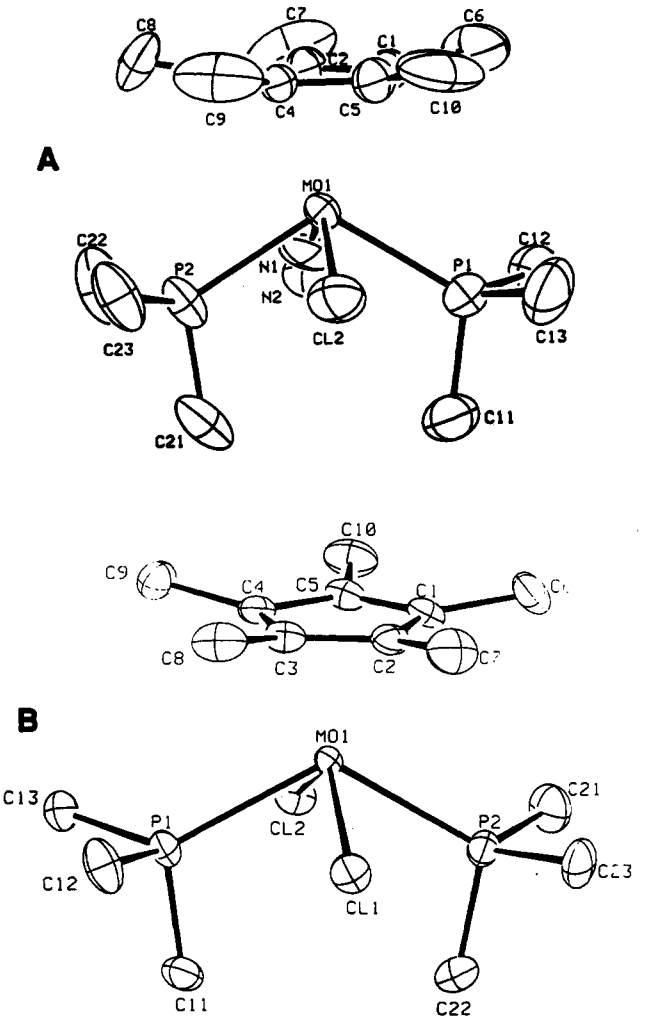

Figure 1. Molecular structures of (A) $Cp^*MoCl(N_2)(PMe_3)_2$ (**1**) and (B) $Cp^*MoCl_2(PMe_3)_2$ (**2**). Hydrogen atoms are omitted for clarity.

The molecular structure of complex **3** (Figure 2) consists also of a four-legged piano stool structure with H trans to Cl (H–W–Cl = 149 (2)°). The C atom of the $(CH_2PMe_2)^-$ ligand is located between the two P atoms in the P–W–P plane. The W–P bond distance to the $(CH_2PMe_2)^-$ ligand (2.35 Å) is significantly shorter than that to PMe_3 (2.48 Å), as observed previously for divalent $WH(PMe_3)_4(\eta^2\text{-}CH_2PMe_2)$ (2.38 vs 2.42–2.45 Å).[14] The W–C_5Me_5 bonding in **3** shows a similar slip distortion (avg W–C11,12 = 2.38 Å, avg W–C13–15 = 2.27 Å) to that found for **1** and **2**.

Spectroscopic Characterization of 1–3. The ^1H and ^{31}P NMR solution spectra (Tables II and III) are consistent with the structure found for **1** in the solid state. In the

(12) Krueger, S. T.; Poli, R.; Rheingold, A. L.; Staley, D. L. *Inorg. Chem.* **1989**, *28*, 4599.

(13) While distortions in related $CpMX_2L_2$ complexes have been attributed to tilting of the Cp ring,[19] the angle between the Cp* ring plane and the best plane containing the Cl and P atoms of **2** is only 3.1°.

(14) Gibson, V. C.; Graimann, C. E.; Hare, P. M.; Green, M. L. H.; Bandy, J. A.; Grebenik, P. D.; Prout, K. *J. Chem. Soc. Dalton Trans.* **1985**, 2025.

Table X. Metal Coordination Geometries for Cp*MXYL(PMe$_3$)[a]

complex	no.	R–M–P	R–M–L	R–M–X	R–M–Y	P–M–L	X–M–Y
Cp*MoCl(N$_2$)(PMe$_3$)$_2$[b]	**1**	124.9	120.7	111.7	116.9	114.4	131.5
Cp*MoCl$_2$(PMe$_3$)$_2$	**2**	121.7	116.6	113.8	115.5	121.6	130.7
Cp*WHCl(η-CH$_2$PMe$_2$)(PMe$_3$)	**3**	122.1	157.2	100	109.6	99.0	149
WH(C$_5$Me$_4$CH$_2$PCy$_2$)(PMe$_3$)$_2$	**6b**	131.5	127.8	103	96.8	97.4	160
Cp*WH(PMe$_3$)(PPh$_2$)$_2$	**8a**	123.0	121.0	93	108.6	113.8	151

[a] Angles in degrees; R = centroid of C$_5$Me$_5$ ring; ligands X, Y, L, and P are defined by the order in which they appear in the complex formula; L for **3** is the centroid of the (η^2-CH$_2$PMe$_2$)$^-$ ligand and Y for **6b** is the PCy$_2$ arm of the (C$_5$Me$_4$CH$_2$PCy$_2$)$^-$ ligand. [b] From orthorhombic crystal structure of ref 11.

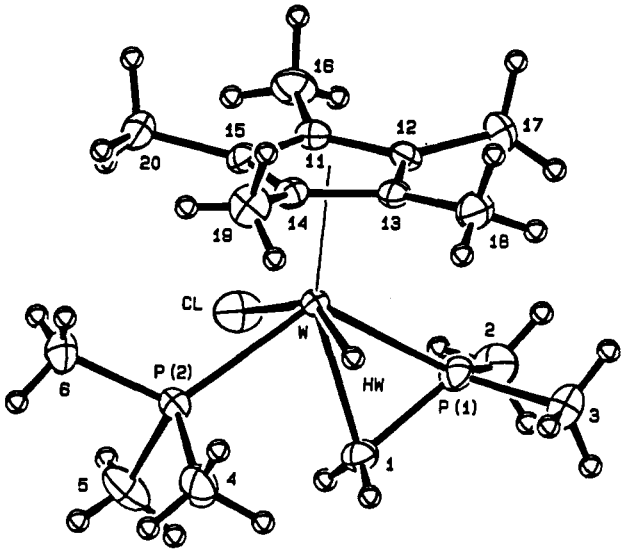

Figure 2. Molecular structure of Cp*WHCl(PMe$_3$)(η^2-CH$_2$-PMe$_2$) (**3**).

IR spectrum, ν_{NN} = 1949 cm^{-1} vs 1950 cm^{-1} for Mo(PMe$_3$)$_5$(N$_2$).[15] Paramagnetic **2** is characterized by broad, temperature-dependent resonances in the ^{1}H NMR at δ 41.8 (Cp*) and −2.5 (PMe$_3$) and a triplet ESR resonance[11] at −100 °C (g_{avg} = 1.9837, $a(^{31}P)$ = 14.9 G, $a(^{95,97}Mo)$ = 35.0 G). For **3**, the tungsten hydride is characterized by ν_{WH} = 1855 cm^{-1} in the IR spectrum and a 16-line doublet of doublet of doublet of doublets with ^{183}W satellites (J_{HW} = 67 Hz) at δ −5.99 in the ^{1}H NMR spectrum, due to coupling to two inequivalent P's ($^2J_{HP}$ = 26, 13 Hz) and the diastereotopic CH$_2$ protons of the (η^2-CH$_2$PMe$_2$)$^-$ ligand ($^3J_{HH}$ = 5.5, 4.5 Hz). The methylene group of the metalated-phosphine ligand shows a characteristic shift to higher field (vs coordinated PMe$_3$) in both the ^{1}H and ^{13}C NMR spectra (Table IV). The ^{31}P NMR spectrum of **3** consists of a pair of doublets ($^2J_{PP}$ = 13.5 Hz) at high field with values of J_{PW} (257, 214 Hz) which are indicative of tetravalent tungsten.[16]

Reactions of 1 and 3 with P(OMe)$_3$, PPh$_2$H, and LiPR$_2$. Complexes **1** and **3** react slowly with P(OMe)$_3$ at 25 °C to give a mixture of purple mixed-ligand products, Cp*MCl[P(OMe)$_3$]$_n$(PMe$_3$)$_{3-n}$ (n = 1, 2; **4a–d**), characterized by ^{31}P and ^{1}H NMR spectroscopy. The ^{31}P NMR spectra of **4a–d** are unchanged at −90 °C, indicating that both mono- and bis[P(OMe)$_3$]-substituted products consist of a single isomer,[17] as shown in Scheme II.

Reactions of **1** and **3** with LiPR$_2$ (R = Ph, Cy) also proceed slowly at 25 °C (Scheme II). While complex **1** gives Cp*Mo(PR$_2$)(PMe$_3$)$_2$ (**5a,b**) as green crystalline solids, **5b** was not obtained analytically pure due to P$_2$Cy$_4$ contamination. Complex **3** yields red-orange crystals of the unusual divalent species (C$_5$Me$_4$CH$_2$PR$_2$)WH(PMe$_3$)$_2$ (**6a,b**) which contain the new functional phosphine ligands[18] (C$_5$Me$_4$CH$_2$PR$_2$)$^-$, arising formally from metal-mediated coupling of tetramethylfulvene and (PR$_2$)$^-$ ligands.

Scheme II

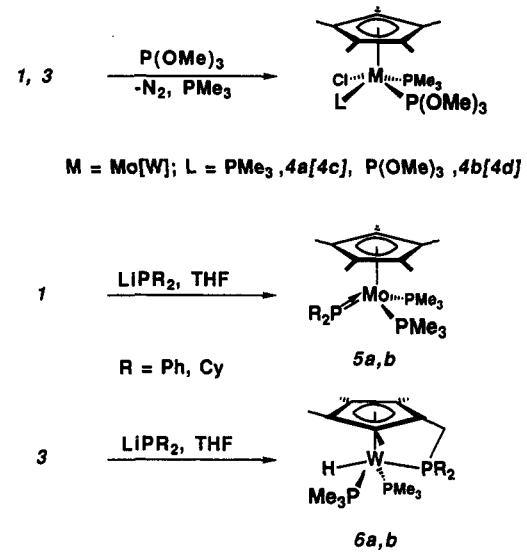

Oxidative addition of PPh$_2$H to complexes **1** and **3** gives the tetravalent complexes Cp*MHCl(PPh$_2$)(PMe$_3$) (**7a,b**) (Scheme III). Complexes **7a,b** react with LiPPh$_2$ to yield green-brown, divalent Cp*Mo(PPh$_2$)(PPh$_2$H)(PMe$_3$) (**5c**) and dark blue, tetravalent Cp*WH(PPh$_2$)$_2$(PMe$_3$) (**8a**). Finally, substitution of the PMe$_3$ ligand in **8a** by PPh$_2$H is accompanied by P–H bond formation, affording green divalent Cp*W(PPh$_2$)(PPh$_2$H)$_2$ (**5e**). Complexes **5–8** were characterized by full elemental analysis, IR and ^{1}H and ^{31}P NMR spectroscopy, and, for **6b** and **8a**, single-crystal X-ray diffraction.

Molecular Structures of 6b and 8a. The molecular structure of **6b** (Figure 3) is a distorted four-legged piano stool with an unusually acute P–W–P angle (97.42 (4)°) between the PMe$_3$ ligands and a large H–W–P′ angle (160 (2)°). This type of distortion has been considered by Hoffmann et al.[19] and will be addressed in the Discussion. The W–C50–C51 angle in the four-membered ring of the

(15) Carmona, E.; Marin, J. M.; Poveda, M. L.; Rogers, R. D.; Atwood, J. L. *J. Organomet. Chem.* **1982**, *238*, C63.

(16) Pregosin, P. S. in *Phosphorus-31 NMR Spectroscopy in Stereochemical Analysis*; Verkade, J. G.; Quin, L. D., Eds.; VCH: Deerfield Beach, FL, 1987; pp 499–500.

(17) The observation of multiple isomers (square pyramidal and trigonal bipyramidal) has been reported for (η-C$_5$H$_5$)MX(CO)L$_2$ (M = Mo, W; X = Cl, Br, I; L = PMePh$_2$, P(OMe)Ph$_2$): Nickias, P. N.; Selegue, J. P. 192nd ACS National Meeting, September, 1986, Anaheim, CA; Abstract INOR 26.

(18) Several related ligands have been reported. [C$_5$Me$_4$P(*p*-tolyl)$_2$]$^-$: Casey, C. P.; Bullock, R. M.; Nief, F. *J. Am. Chem. Soc.* **1983**, *105*, 7574. [C$_5$Me$_4$CHMePPh$_2$]$^-$: Bensley, D. M.; Mintz, E. A. *J. Organomet. Chem.* **1988**, *353*, 93.

(19) Kubacek, P.; Hoffmann, R.; Havlas, Z. *Organometallics* **1982**, *1*, 180.

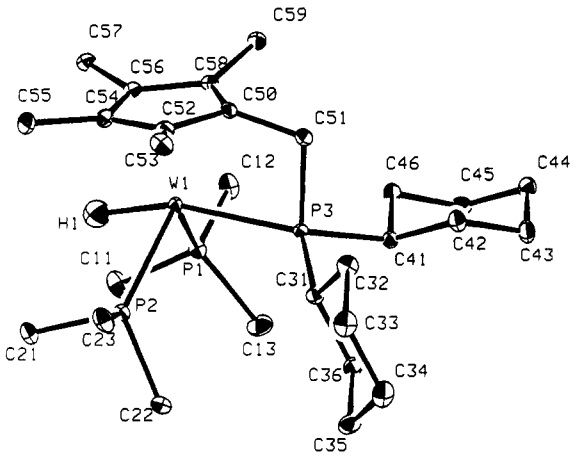

Figure 3. Molecular structure of $(C_5Me_4CH_2PCy_2)WH(PMe_3)_2$ (**6b**). Hydrogen atoms are omitted for clarity.

Scheme III

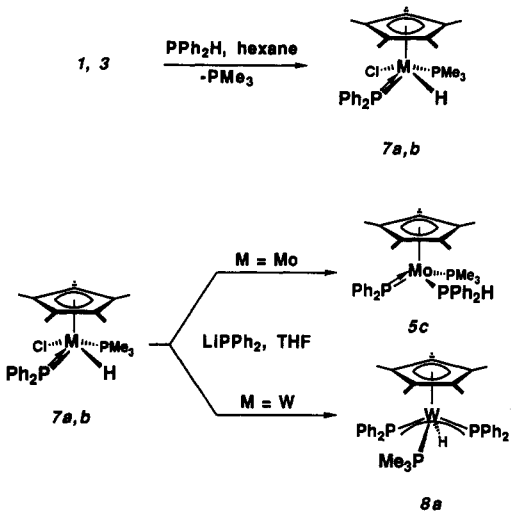

chelated $(C_5Me_4CH_2PCy_2)^-$ ligand is 105.8° vs 128–134° for the four W–C–CH_3 angles. In contrast to **3**, the W atom in **6b** is located directly above the centroid of the Cp* ring. The molecular structure of **8a** (Figure 4) contains "trans" $(PPh_2)^-$ ligands (P2–W–P3) = 113.8°). The W–P bond distances (avg 2.324 (2) Å) are shorter than those reported for $[W(PBu^t_2)(NMe_2)_2]_2$ (2.398 (2) Å)[20] and for $TaH(PPh_2)_2(DMPE)_2$ (avg 2.417 (6) Å),[21] but not so short as that found for $CpW(CO)_2(PPr^i_2)$ (2.284 (4) Å),[22] in which the $(PR_2)^-$ ligand is a 4e$^-$ donor. Most notable, however, is the pseudoparallel orientation of the $(PPh_2)^-$ ligand PC^{ipso}_2 planes[23] relative to the plane of the C_5Me_5 ring. These observations suggest that W and the two "trans" $(PPh_2)^-$ ligands form a pseudoallylic bonding unit with W–P bond orders of 1.5 (see later discussion). The W–C_5Me_5 bonding in **8a** shows a slip distortion in the opposite sense to that seen for **1–3** (avg W–C3,4 = 2.30 Å; avg W–C1,2,5 = 2.39 Å). Similar distortions were observed by Poli et al. in trivalent $CpMoCl_2(PMe_3)_2$[12a] and $CpMoBr_2(DPPE)$.[12b]

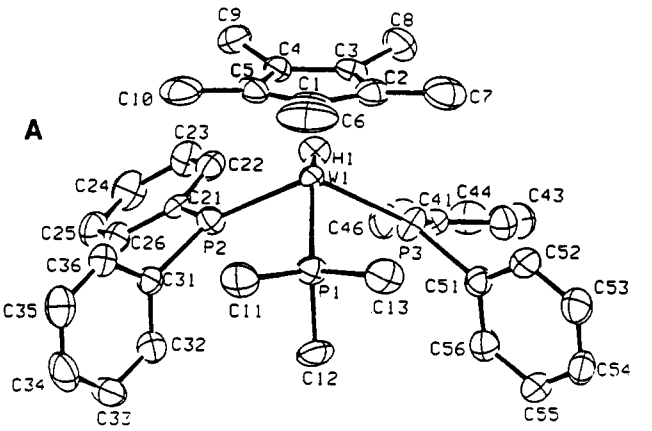

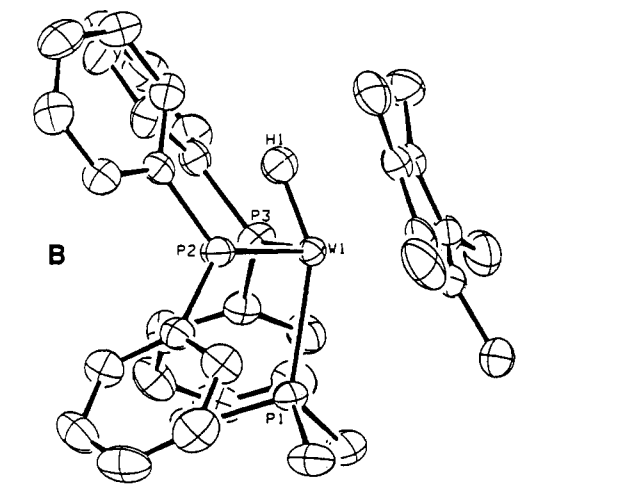

Figure 4. Molecular structure of $Cp^*WH(PPh_2)_2(PMe_3)$ (**8a**) showing the orientation of the PC^{ipso}_2 planes (A) and viewed along the P2–W–P3 plane (B). Hydrogen atoms are omitted for clarity.

Spectroscopic Characterization of 4–8. The ^{31}P NMR spectra of $Cp^*MCl[P(OMe)_3]_n(PMe_3)_{3-n}$ (**4a–d**) indicate that substitution of N_2 and one PMe_3 ligand in **1** and **3** gives a single stereoisomer for both mono- and bis(phosphite) complexes. Complexes **5a,b** are analogous to previously reported $(\eta$-$C_5R_5)M(CO)_2(PR'_2)$ complexes (R = H, Me; M = Mo, W; R' = Bu^t, Pr^i)[22] and are characterized by a low-field ^{31}P NMR chemical shift due to the planar $(PR_2)^-$ ligand (triplet at 161.3 and 238.7 ppm for **5a,b**, respectively). Analogous low-field shifts are also observed for divalent $Cp^*WL(PPh_2)(PPh_2H)$ (**5d,e**) (137.4 and 155.2 ppm) and tetravalent $Cp^*MHCl(PPh_2)(PMe_3)$ (**7a,b**) (220.2 and 145.1 ppm). Consistent with our electronic structural proposal (see discussion below), chemical shifts of the $(PPh_2)^-$ ligands in tetravalent $Cp^*WHL(PPh_2)_2$ (**8a,b**) appear at higher field (98.8, 105.8 ppm) due to reduced P→W π-donation. Isolation of divalent **5e** from the reaction of tetravalent **8a** with PPh_2H suggests that these tautomeric structures are of comparable stability. In fact, NMR spectra indicate that **8a** is in equilibrium (K_{298} = ca. 1) with its divalent tautomer $Cp^*W(PPh_2)(PPh_2H)(PMe_3)$ (**5d**), thus providing the first example of simple, reversible P–H bond activation[24] (Scheme IV). For the **8b**/**5e** equilibrium, divalent **5e** is the major tautomer (K_{298} = ca. 18), as expected from phosphine basicity arguments. The $^2J_{HP}$ values observed for the W–H resonance in the ^1H NMR spectra of **6a,b** show larger "cis" couplings (57, 58 Hz) than "trans" (13, 12.5 Hz), as reported previously for the equatorial W–H

(20) Buhro, W. E.; Chisholm, M. H.; Folting, K.; Huffman, J. C.; Martin, J. D.; Streib, W. E. *J. Am. Chem. Soc.* **1992**, *114*, 527.
(21) Domaille, P. J.; Foxman, B. M.; McNeese, T. J.; Wreford, S. S. *J. Am. Chem. Soc.* **1980**, *102*, 4114.
(22) Jorg, K.; Malisch, W.; Reich, W.; Meyer, A.; Schubert, U. *Angew. Chem. Intl. Ed. Engl.* **1986**, *25*, 92.
(23) Sum of the angles about P2 and P3 are 359.9 and 359.2°, respectively.

Scheme IV

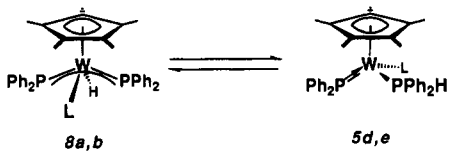

Scheme V

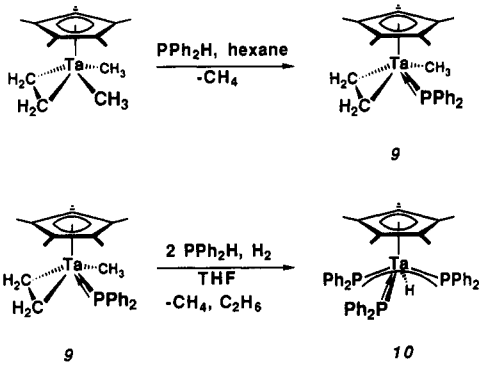

in $[CpWH_2(PMe_3)_3]^+$ ($^2J_{HP}$ = 40 vs 8.5 Hz).[25] A similar trend is observed for **8a**. For **7a,b** the M–H gives rise to a doublet of doublets at δ −3.29 (−3.12) with $^2J_{HP}$ = 95 (83) and 54.5 (44) Hz for the Mo (W) analog. These data suggest that H is trans to Cl in **7a,b** and the ^{1}H-coupled ^{31}P NMR spectra show the larger coupling is due to the PMe_3 ligand. The P–H functionality is characterized in the ^{1}H NMR spectra of **5c–e** by a doublet of doublets resonance at δ 8.31 (J_{HP} = 306), 10.34 (316), and 10.09 (328), respectively, due to a three-bond coupling (6 Hz for **5c,d**, 14.5 Hz for **5e**) to the $(PPh_2)^-$ ligand. By IR spectroscopy, the M–H's are observed at 1855, 1895 cm^{-1} for **6a,b**, and 1833, 1855 cm^{-1} for **7a,b**; ν_{WH} is not observed for **8a**. The P–H's give rise to a strong absorption at 2232 cm^{-1} for both **5c,e**.

Synthesis and Spectroscopic Characterization of Cp*Ta Complexes, 9 and 10. Reaction of $Cp^*TaMe_2(\eta\text{-}C_2H_4)$ with PPh_2H gives orange crystals of $Cp^*TaMe(PPh_2)(\eta\text{-}C_2H_4)$ (**9**) with evolution of methane. Larger secondary phosphines such as PCy_2H gave no reaction, while PEt_2H reacted with $Cp^*TaMe_2(\eta\text{-}C_2H_4)$ to give PEt_2-bridged products which were not characterized further. Although excess PPh_2H did not react readily with **9** either thermally or photochemically, hydrogenolysis of **9** in the presence of 2 equiv of PPh_2H afforded purple crystals of $Cp^*TaH(PPh_2)_3$ (**10**) in good yield (Scheme V). Complexes **9** and **10** were characterized by full elemental analysis and IR and NMR spectroscopy. The ^{31}P NMR spectrum of **9** contains a low-field resonance at 170.3 ppm, indicative of a multiply bonded, trigonal-planar $(PR_2)^-$ ligand. Barriers to rotation about Ta–P (11.6 ± 0.3 kcal/mol) and Ta–olefin bonds (>15 kcal/mol) in **9** were conveniently estimated from ^{13}C DNMR spectra (Figure 5). The ^{31}P NMR spectrum of **10** at −80 °C consists of a triplet at 253.2 and a doublet at 119.6 ppm ($^2J_{PP}$ = 59 Hz). At 110 °C a single broad resonance is observed at 169 ppm (Figure 6). In the ^{1}H NMR spectrum, the quartet Ta–H resonance ($^2J_{HP}$ = 65 Hz) observed at δ 9.90 at 25 °C (Figure 7) becomes a triplet of doublets at −90 °C ($^2J_{HP}$ = 84, 25 Hz). On the basis of ^{31}P NMR chemical shifts and the fact that **10** and **8** are isoelectronic, we propose that **10** also has the pseudoallylic, delocalized P–Ta–P bonding system with the PC^{ipso}_2 planes of the $(PPh_2)^-$ ligands roughly parallel to the C_5Me_5 ring plane. In **10**, however, we also have one doubly bonded, trigonal-planar $(PPh_2)^-$ ligand with its PC^{ipso}_2 plane *perpendicular* to the C_5Me_5 ring plane. The dynamic process which equilibrates these two types of $(PPh_2)^-$ ligands is proposed to involve a distorted-trigonal-bipyramidal intermediate[19] (Scheme VI). The Ta–H stretching vibration is not observed in the IR spectrum of **10** (cf. the IR-silent W–H in **8a**).

Scheme VI

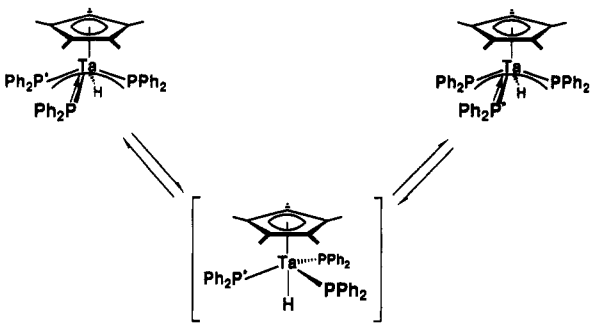

Discussion

Synthesis. Reduction of $Cp^*MCl_4(PMe_3)$ in the presence of PMe_3 provides a convenient entry into Cp*Mo and Cp*W PMe_3 chemistry. While the electron-rich nature of $Cp^*MoCl(N_2)(PMe_3)_2$ (**1**) stabilizes the M–N_2 linkage,[26] substitution reactions with sterically undemanding ligands such as $P(OMe)_3$ proceed readily. Addition of ligands to $Cp^*WHCl(PMe_3)(\eta\text{-}CH_2PMe_2)$ (**3**) to give divalent $Cp^*WClL(PMe_3)_2$ is also facile, as phosphine metalation is easily reversible. Complexes **1** and **3** both undergo oxidative addition and Cl^- metathesis reactions as shown for PPh_2H and $LiPR_2$, respectively. Oxidative addition reactions of PPh_2H are accompanied by loss of a PMe_3 ligand in order to accommodate the resulting 4e$^-$ donor $(PPh_2)^-$ ligand. This behavior is intermediate between conventional addends, such as alkyl halides, and those which lead to two multiply bonded ligands upon addition, such as Bryan and Mayer's reactions[27] of $WCl_2(PMePh_2)_4$ with CO_2 and R_2CO to give $WOCl_2(CO)(PMePh_2)_2$ and $WOCl_2(CR_2)(PMePh_2)_2$.

While activation of PMe_3 and $(C_5Me_5)^-$ ligand sp^3 C–H bonds has been observed in other electron-rich W complexes,[14,28] the reaction of **3** with $LiPR_2$ is an unusual example of ring functionalization by metal-mediated P–C bond formation.[29,32] We assume the divalent W center in the $[Cp^*W(PR_2)(PMe_3)_n]$ (n = 1 or 2) intermediate attacks

(24) A previously reported example of reversible P–H bond activation was coupled with ancillary ligand binding, i.e. $(PCy_2)(PCy_2H)(N_2)Re(\mu\text{-}PCy_2)_2Pd(PPh_3) \rightleftharpoons N_2 + (PCy_2)_2ReH(\mu\text{-}PCy_2)_2Pd(PPh_3)$: Baker, R. T.; Glassman, T. E.; Calabrese, J. C. *Organometallics* **1988**, *7*, 1889. Also, the addition of PH_3 to $[Ir(DPPE)_2]BPh_4$ to give $[IrH(PH_2)(DPPE)_2]BPh_4$ is reversed in refluxing acetonitrile: Schunn, R. A. *Inorg. Chem.* **1973**, *12*, 1573.

(25) Green, M. L. H.; Parkin, G. *J. Chem. Soc. Dalton Trans.* **1987**, 1611.

(26) Methylation of **1** by methyllithium in hexane proceeds with retention of the N_2 ligand to give $Cp^*MoMe(N_2)(PMe_3)_2$. Baker, R. T., unpublished results.

(27) Bryan, J. C.; Geib, S. J.; Rheingold, A. L.; Mayer, J. M. *J. Am. Chem. Soc.* **1987**, *109*, 2826. Bryan, J. C.; Mayer, J. M. *ibid.* **1987**, *109*, 7213; *ibid.* **1990**, *112*, 2298; *Polyhedron* **1989**, *8*, 1261.

(28) Cloke, F. G. N.; Green, J. C.; Green, M. L. H.; Morley, C. P. *J. Chem. Soc., Chem. Commun.* **1985**, 945.

(29) Dobbie, R. C.; Green, M.; Stone, F. G. A. *J. Chem. Soc. A* **1969**, 1881. Related reactions include insertion of unsaturated hydrocarbon fragments into the M–PR_2 bond[30] and metal-mediated hydrophosphination of alkenes and carbonyl compounds.[31]

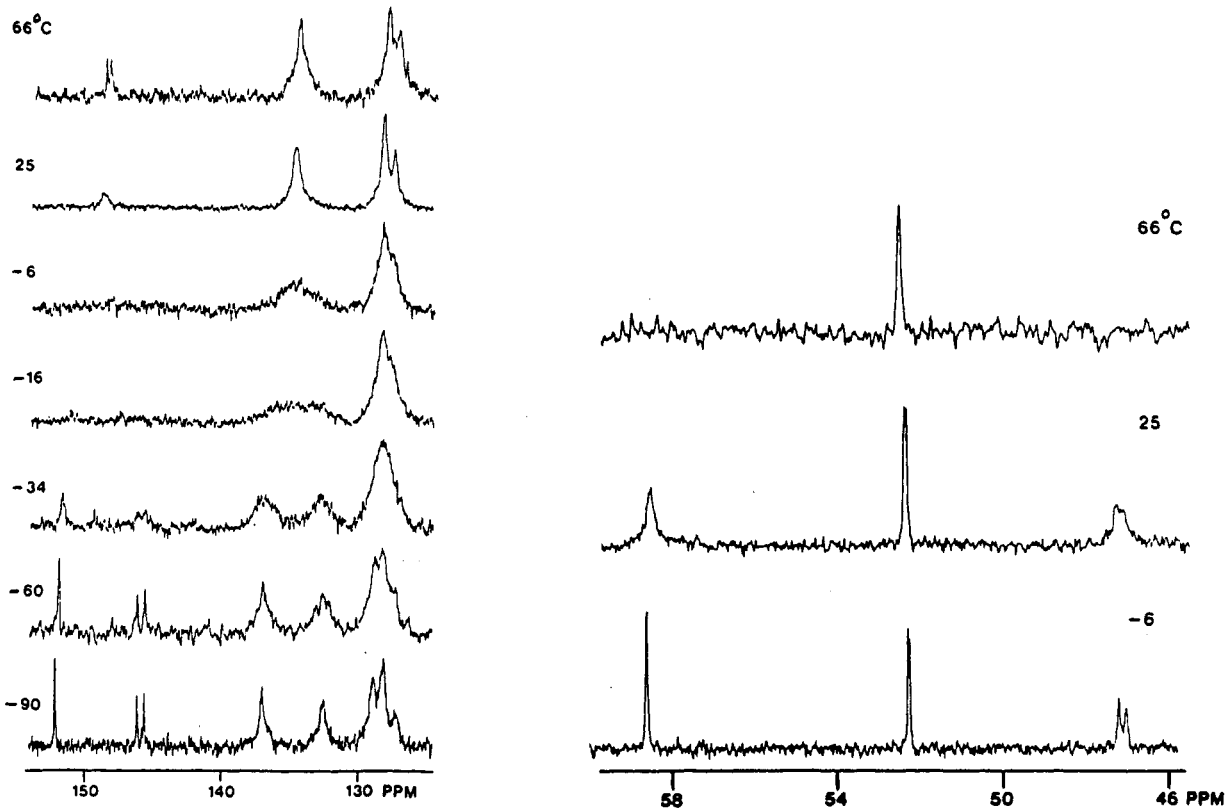

Figure 5. ^{13}C DNMR spectra of Cp*TaMe(PPh_2)(η-C_2H_4) (**9**) in THF-d_8.

the Cp* ring methyl to give "tuck-in" hydride [(η^6-$C_5Me_4CH_2$)$WH(PR_2)(PMe_3)_n$], which subsequently eliminates to form ($C_5Me_4CH_2PR_2$)$WH(PMe_3)_2$ (**6a,b**). Note that divalent Cp*$W(PR_2)L_2$ complexes are stable when L is a π-acceptor ligand such as CO[22] or even a poorer donor than PMe_3 such as PPh_2H (cf. **5d,e**). Complexes **5d,e** also provide the first examples of reversible P–H bond activation without dissociation of an ancillary ligand.[24] Equilibria between **5d,e** and their tetravalent tautomers Cp*$WHL(PPh_2)_2$ (**8a,b**) favor the former when L = PPh_2H and is ca. 1 for the stronger electron donor PMe_3. Although reaction of tetravalent Cp*$MoHCl(PPh_2)(PMe_3)$ with $LiPPh_2$ affords divalent Cp*$Mo(PPh_2)(PPh_2H)(PMe_3)$ (**5c**), both **5c** and **8a** react readily with CpPd(2-Me-allyl)/PPh_3 to give doubly bonded heterobimetallics Cp*$MH(PMe_3)(\mu$-$PPh_2)_2Pd(PPh_3)$ as reported elsewhere.[5,33]

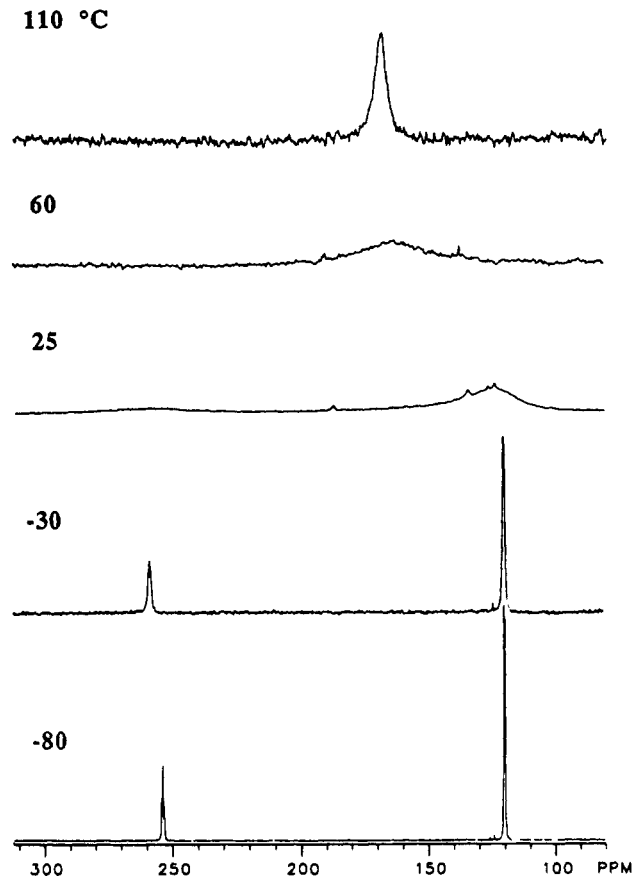

Figure 6. ^{31}P DNMR spectra of Cp*$TaH(PPh_2)_3$ (**10**) in toluene-d_8.

The synthesis of Cp*$TaMe(PPh_2)(\eta$-$C_2H_4)$ (**9**) is facilitated by use of 14e⁻ precursor Cp*$TaMe_2(\eta$-$C_2H_4)$, which is prepared conveniently from $TaCl_5$ in three steps.[8] Steric crowding about the Ta center in 16e⁻ **9** presumably

(30) Smith, W. F.; Taylor, N. J.; Carty, A. J. *J. Chem. Soc., Chem. Commun.* **1976**, 896; Regragui, R.; Dixneuf, P. H.; Taylor, N. J.; Carty, A. J. *Organometallics* **1984**, *3*, 814; Werner, H.; Zolk, R. *Chem. Ber.* **1987**, *120*, 1003; Rosenberg, S.; Whittle, R. R.; Geoffroy, G. L. *J. Am. Chem. Soc.* **1984**, *106*, 5934; Horton, A. D.; Mays, M. J.; Raithby, P. R. *J. Chem. Soc., Chem. Commun.* **1985**, 247; Henrick, K.; McPartlin, M.; Iggo, J. A.; Kemball, A. C.; Mays, M. J.; Raithby, P. R. *J. Chem. Soc. Dalton Trans.* **1987**, 2669; Conole, G.; McPartlin, M.; Mays, M. J.; Morris, M. J. *J. Chem. Soc. Dalton Trans.* **1990**, 2359.

(31) Bartch, R.; Kietkamp, S.; Morton, S.; Peters, H.; Stelzer, O. *Inorg. Chem.* **1983**, *22*, 3625; Harrison, K. N.; Hoye, P. A. T.; Orpen, A. G.; Pringle, P. G.; Smith, M. B. *J. Chem. Soc., Chem. Commun.* **1989**, 1096; Pringle, P. G.; Smith, M. B.; *ibid.* **1990**, 1701; Bohle, D. S.; Clark, G. R.; Rickard, C. E. F.; Roper, W. R. *J. Organomet. Chem.* **1990**, *393*, 243; Giardello, M. A.; King, W. A.; Nolan, S. P.; Porchia, M.; Sishta, C.; Marks, T. J. in *Energetics of Organometallic Species*, Martinho Simoes, J. A., Ed., Kuwer:Dordrecht, **1992**, pp. 35–51.

(32) Observation of metal-mediated P–C bond cleavage is much more common: Garrou, P. E.; *Chem. Rev.* **1985**, *85*, 171 and references contained therein. Particularly relevant to this work is the photochemical hydrogenolysis of [η^5-$C_5H_4P(p$-tol)$_2$]$Mo(CO)_3Mn(CO)_4$ to $CpMo(CO)_2(\mu$-H)-[μ-$P(p$-tol)$_2$]$Mn(CO)_4$. Casey, C. P.; Bullock, R. M. *Organometallics* **1984**, *3*, 1100.

(33) Baker, R. T.; Calabrese, J. C., International Symposium on Polymetallic Activation, Parma, Italy, September, **1990**. See also Braunstein, P. *Platinum Metals Review* **1991**, *35*, 10.

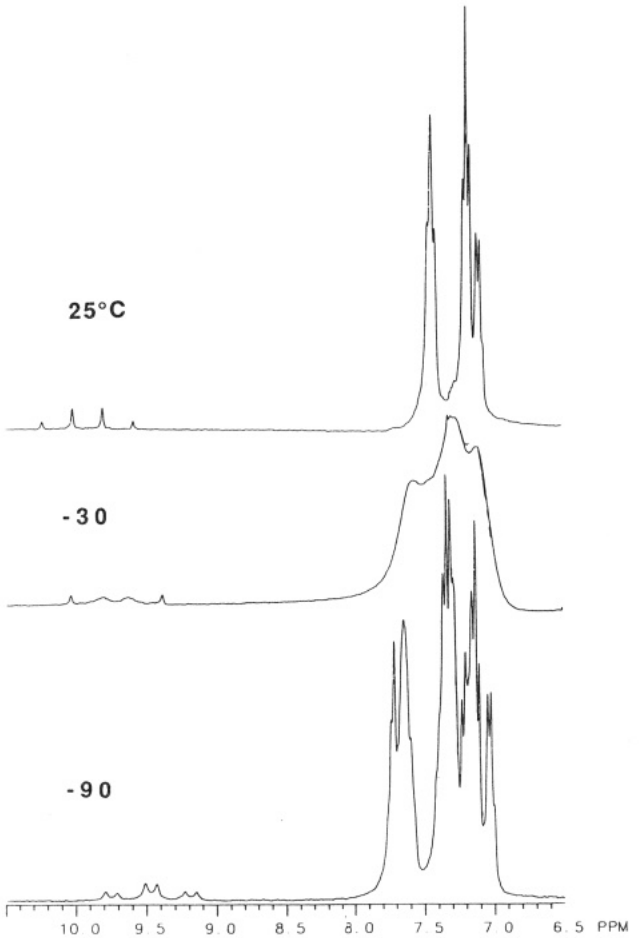

Figure 7. ^{1}H DNMR spectra of Cp*TaH(PPh_2)$_3$ (**10**) in toluene-d_8.

disfavors coordination of a second molecule of PPh_2H. The stability of d^0 Cp*TaH(PPh_2)$_3$ (**10**) under H_2 is in marked contrast to the ease of hydrogenation of [Re≡PCy_2] to [ReH(PCy_2H)] in several d^2 and d^4 complexes.[34] Complex **10** is a versatile metallo ligand, functioning in both bidentate (Cp*TaH(PPh_2)(μ-PPh_2)$_2$Pd(PPh_3)) and tridentate modes (Cp*TaH(μ-PPh_2)$_3$RhH(PMe_3)).[33] Details of the construction and molecular structures of unsaturated heterobimetallics from **5c**, **8a**, and **10** will be described separately.[35]

Molecular Structures. Molecular and electronic structures of $CpML_4$ piano stool complexes have been analyzed in detail by Hoffmann et al.[19] and more recently by Poli.[36] While the steric bulk of the $(C_5Me_5)^-$ ligand may mask some of the subtle electronic effects observed by Poli in Cp complexes, it can also exaggerate distortions from typical square-pyramidal geometry. The 14e$^-$ cation $[Cp^*WMe_4]^+$, for example, is the only structurally characterized, trigonal-bipyramidal $CpML_4$ analog with an axial ring.[37] Additionally, the very large angles from the ring centroid to the PMe_3 ligands (avg 130°) and the large

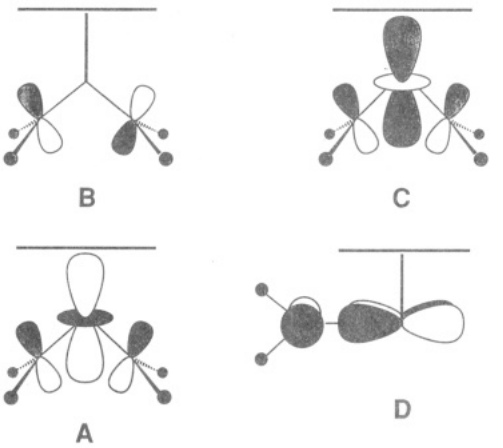

Figure 8. The idealized bonding (A), nonbonding (B), and antibonding (C) components of the pseudoallylic [M(PPh_2)$_2$] moiety in Cp*WH(PPh_2)$_2$(PMe_3) (**8a**) and Cp*TaH(PPh_2)$_3$ (**10**) and the additional Ta–P π-bond (D) in **10**.

H–W–P (160°) and small P–M–P angles (97°) observed for ($C_5Me_4CH_2PCy_2$)WH(PMe_3)$_2$ (**6b**) are as predicted by Hoffmann[19] for a tbp structure with an *equatorial* ring. This distortion may also be caused by the necessarily small angle from the C_5Me_5 ring centroid to the PCy_2 arm of the chelating $(C_5Me_4CH_2PCy_2)^-$ ligand (see also Note Added in Proof).

Hoffmann et al. noted also[19] that optimal π-bonding interactions between M and L are a sensitive function of the ring-centroid–M–L angle, θ. For θ = 90°, a single-faced, π-bonding ligand such as $(PPh_2)^-$ will be oriented with the PC^{ipso}_2 plane perpendicular to the ring plane to ensure maximum overlap with the metal d_{xy} orbital. For θ = 135°, the ligand plane will be pseudoparallel to the ring plane to attain optimal overlap with the metal d_{z^2} orbital. In 18e$^-$ d^4 $CpML_4$ complexes, the highest and second highest occupied molecular orbitals are mostly metal z^2 and xy, respectively. For d^2 Cp*WH(PPh_2)$_2$(PMe_3) (**8a**) the xy orbital is filled and the empty z^2 orbital can then interact with the four electrons from the two π-donor $(PPh_2)^-$ ligands in a pseudoallylic bonding arrangement with one bonding, one nonbonding, and one antibonding molecular orbital (Figure 8A–C). Consistent with this picture, the average angle θ to the $(PPh_2)^-$ ligands is 122° (vs 109° to PMe_3) and the PC^{ipso}_2 planes are pseudoparallel to the C_5Me_5 ring plane. For d^0 Cp*TaH(PPh_2)$_3$ (**10**) the xy orbital is also empty, allowing the formation of an additional Ta–P multiple bond in which the PC^{ipso}_2 plane is now perpendicular to the ring plane (Figure 8D). While the molecular structure of **10** has not been determined, a similar Ta–P multiple bond in the bimetallic complex Cp*TaH(PPh_2)(μ-PPh_2)$_2$Pt(PPh_3) has a θ angle of 121°, in spite of the proximity of the C_5Me_5 ring methyl hydrogens to one of the phenyl rings of the terminal $(PPh_2)^-$ ligand.[35] For three-legged piano stools such as Cp*TaMe(PPh_2)(η-C_2H_4) (**9**), the bonding situation is complicated by significant mixing between orbitals engaged in σ- and π-bonding.[38] If we assume the coordinated alkene and the (C_5Me_5) ring plane are in a pseudoparallel orientation (cf. the structure of 14e$^-$ Cp*TaCl$_2$(η-CH$_2$=CH$_2$)[39]), however, we can formally consider **9** to be a 16e$^-$ d^0 metallacyclopropane complex

(34) Baker, R. T.; Glassman, T. E.; Ovenall, D. W.; Calabrese, J. C. *Isr. J. Chem.* **1991**, *31*, 33.
(35) Baker, R. T.; Calabrese, J. C.; Harlow, R. L.; Ovenall, D. W., manuscript in preparation.
(36) Poli, R. *Organometallics* **1990**, *9*, 1892.
(37) Liu, A. H.; Murray, R. C.; Dewan, J. C.; Santarsiero, B. D.; Schrock, R. R. *J. Am. Chem. Soc.* **1987**, *109*, 4282. The methyl groups in the $[Cp^*WMe_4]^+$ cation were badly disordered, however, and recent NMR studies indicate that the ground state structure includes an agostic W-H-C interaction involving one of the equatorial methyls. Green, M. L. H.; Hughes, A. K.; Popham, N. A.; Stephens, A. H. H.; Wong, L.-L. *J. Chem. Soc., Dalton Trans.* **1992**, 3077.
(38) Albright, T. A.; Burdett, J. K.; Whangbo, M.-H. *Orbital Interactions in Chemistry*; John Wiley and Sons: New York, 1984.
(39) Youngs, W. J.; Churchill, M. R. unpublished results, cited as ref 19 in Churchill, M. R.; Youngs, W. J. *Inorg. Chem.* **1980**, *19*, 3106.

and a four-legged piano stool. Following the above arguments (donation from $p\pi \rightarrow d_{xy}$ with d_{z^2} empty), the 4e⁻ donor $(PPh_2)^-$ ligand would then be expected to adopt a perpendicular orientation with respect to the ring plane. The above assumption may be risky, however, as the acceptor orbitals are likely to be close in energy[40] and lack of symmetry may affect the observed conformations.[41]

While the correlation of ^{31}P chemical shifts supports the presence of both double (253.2 ppm) and partial (119.6 ppm) Ta–P multiple bonds in $Cp^*TaH(PPh_2)_3$ (**10**), the best indicator of M–P multiple bonding is the one-bond M–P coupling constant.[20,22] Thus, while J_{PW} = 640, 643 Hz for the 4e⁻ donor $(PPh_2)^-$ ligand in divalent $Cp^*WL(PPh_2)(PMe_3)$ (**5d,e**) and 558 Hz for tetravalent $Cp^*WHCl(PPh_2)(PMe_3)$ (**7b**), for tetravalent $Cp^*WHL(PPh_2)_2$ (**8a,b**), for which W–P bond orders of 1.5 are proposed, J_{PW} is only 369, 350 Hz. Compare this with J_{PW} = 207, 263 Hz in trivalent *anti*- and *gauche*-1,2-$W_2(PPh_2)_2(NMe_2)_4$ in which the terminal diphenylphosphide ligands are pyramidal about phosphorus.[20]

Conclusions

New complexes $Cp^*MoCl(N_2)(PMe_3)_2$ (**1**) and $Cp^*WHCl(PMe_3)(\eta$-$CH_2PMe_2)$ (**3**) are good preparative sources of "$Cp^*MCl(PMe_3)_2$", and both readily undergo ligand addition and/or substitution, Cl^-/X^- metathesis, and oxidative addition reactions. Formal substitution of PPh_2H in $Cp^*W(PPh_2)(PPh_2H)_2$ (**5e**) by PMe_3 ligands gives $Cp^*WH(PPh_2)_2(PMe_3)$ (**8a**), which equilibrates with its tautomer $Cp^*W(PPh_2)(PPh_2H)(PMe_3)$ (**5d**) via P–H bond activation, and finally $(C_5Me_4CH_2PPh_2)WH(PMe_3)_2$ (**6a**) which arises by Cp* ring methyl C–H bond activation, followed by P–C bond formation. Hydrogenolysis of $Cp^*TaMe(PPh_2)(\eta$-$C_2H_4)$ (**9**) in the presence of PPh_2H gives $Cp^*TaH(PPh_2)_3$ (**10**). Complexes **5**, **8**, and **10** are convenient multidentate metallo ligands for construction of early–late heterobimetallic complexes.

Note Added in Proof. The geometric distortions observed for the d^4 four-legged piano stool complexes **1** and **6b** are consistent with the "σ-interaction" model put forward recently (Lin, Z.; Hall, M. B. *Organometallics* **1993**, *12*, 19).

Acknowledgment. We thank the following people for fine technical assistance: synthesis, T. J. Onley, G. M. DiRenzo; NMR, E. A. Conaway; X-ray, W. J. Marshall, L. F. Lardear, and Professor Nancy L. Jones (LaSalle). We also thank Professors J. V. Ortiz (New Mexico), R. Poli (Maryland), W. E. Crowe (Emory), and M. L. H. Green (Oxford) for valuable discussions.

Supplementary Material Available: A table of IR spectroscopic data for all new isolated compounds and, for **1–3**, **6b**, and **8a**, tables of final positional and thermal parameters for non-hydrogen atoms, general temperature factors, calculated hydrogen atom positions, and complete listings of bond distances and angles (45 pages). Ordering information is given on any current masthead page.

OM9205051

(40) While the 4e donor acetylene ligand in $Cp^*TaCl_2(\eta$-$C_2Ph_2)$ is oriented parallel to the C_5Me_5 ring plane (Smith, G.; Schrock, R. R.; Churchill, M. R.; Youngs, W. J. *Inorg. Chem.* **1981**, *20*, 387), in the analogous benzyne complex a perpendicular orientation is observed. Churchill, M. R.; Youngs, W. J. *Inorg. Chem.* **1979**, *18*, 1697.

(41) Schilling, B. E. R.; Hoffmann, R.; Faller, J. W. *J. Am. Chem. Soc.* **1979**, *101*, 592.

(42) Schrock, R. R.; Sharp, P. R. *J. Am. Chem. Soc.* **1978**, *100*, 2389.